WL-TR-97-3107

VERIFICATION OF LIFE PREDICTION METHODS FOR AGING AIRCRAFT STRUCTURES

J.H. Elsner, K.L Boyd
Analytical Services and Materials, Inc.
107 Research Drive
Hampton, Virginia 23666

J.A. Harter
WL/FIBE, BLDG 65
2790 D St. Rm. 504
Wright-Patterson AFB, OH 45433-7402

Final Report for Period 01 April 1996 – 31 March 1997
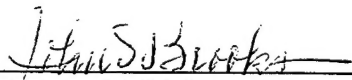
August 1997

DTIC QUALITY INSPECTED 2

19980317 125

NOTICE

USING GOVERNMENT DRAWINGS, SPECIFICATIONS, OR OTHER DATA INCLUDED IN THIS DOCUMENT FOR ANY PURPOSE OTHER THAN GOVERNMENT PROCUREMENT DOES NOT IN ANY WAY OBLIGATE THE US GOVERENMENT. THE FACT THAT THE GOVERNMENT FORMULATED OR SUPPLIED THE DRAWINGS, SPECIFICATIONS, OR THER DATA DOES NOT LICENSE THE HOLDER OR ANY OTHER PERSON OR CORPORATION; OR CONVEY ANY RIGHTS OR PERMISSION TO MANUFACTURE, USE, OR SELL ANY PATENTED INVENTION THAT MAY RELATE TO THEM.

THIS REPORT IS RELEASABLE TO THE NATIONAL TECHNICAL INFORMATION SERVICE (NTIS). AT NTIS, IT WILL BE AVAILABLE TO THE GENERAL PUBLIC, INCLUDING FOREIGN NATIONS.

THIS TECHNICAL REPORT HAS BEEN REVIEWED AND IS APPROVED FOR PUBLICATION.

JOHN S. BROOKS
TEAM LEADER
STRUCTURAL INTEGRITY BRANCH

JAMES A. HARTER
AEROSPACE ENGINEER
STRUCTURAL INTEGRITY BRANCH

JOHN T. ACH
BRANCH CHIEF
STRUCTURAL INTEGRITY BRANCH

IF YOUR ADDRESS HAS CHANGED, IF YOU WISH TO BE REMOVED FROM OUR MAILING LIST, OR IF THE ADDRESSEE IS NO LONGER EMPLOYED BY YOUR ORGANIZATION, PLEASE NOTIFY WL/FIBE, BLDG 65, 2790 D ST., ROOM 504, WRIGHT-PATTERSON AFB OH 45433-7402 TO HELP MAINTAIN A CURRENT MAILING LIST.

Do not return copies of this report unless contractual obligations or notice on a specific document requires its return.

REPORT DOCUMENTATION PAGE		**Form Approved OMB No. 0704-0188**

1. AGENCY USE ONLY *(Leave blank)*	2. REPORT DATE August 1997	3. REPORT TYPE AND DATES COVERED FINAL, 1 Apr 96 - 31 Mar 97	

4. TITLE AND SUBTITLE
Verification of Life Prediction Methods for Aging Aircraft Structures

6. AUTHOR(S)

J.H. Elsner and K. L. Boyd - Analytical Services & Materials, Inc.
J. A. Harter - WL/FIBE

5. FUNDING NUMBERS
C - F33615-94-D-3212
PE - 62201
PR - 2401
TA - 01
WU - 01

7. PERFORMING ORGANIZATION NAME(S) AND ADDRESS(ES)

ANALYTICAL SERVICES AND
MATERIALS, INC.
107 RESEARCH DRIVE
HAMPTON VA 23666

FLIGHT DYNAMICS DIRECTORATE
WRIGHT LABORATORY
AIR FORCE MATERIEL COMMAND
WPAFB, OH 45433-7402

8. PERFORMING ORGANIZATION REPORT NUMBER

9. SPONSORING/MONITORING AGENCY NAME(S) AND ADDRESS(ES)
FLIGHT DYNAMICS DIRECTORATE
WRIGHT LABORATORY
AIR FORCE MATERIEL COMMAND
WRIGHT-PATTERSON AFB OH 45433-7562
POC: JOHN BROOKS, WL/FIBE, 937-255-6104 X 233

10. SPONSORING/MONITORING AGENCY REPORT NUMBER

WL-TR-97-3107

11. SUPPLEMENTARY NOTES

12a. DISTRIBUTION AVAILABILITY STATEMENT
APPROVED FOR PUBLIC RELEASE;
DISTRIBUTION UNLIMITED

12b. DISTRIBUTION CODE

13. ABSTRACT *(Maximum 200 words)*
The purpose of this research is to verify methodologies for AFGROW developed in conjunction with Delivery Order 0006, Contract F33615-94-D-3212. The methodologies, which pertain to aging aircraft, include bonded repair of metallic structures, widespread fatigue damage, stress level effects on crack growth and load sequence effects on crack growth. AFGROW is a fatigue crack growth prediction code developed by Analytical Services and Materials, Inc. and the Air Force

This research is necessitated by the growing need to keep current aircraft in service well beyond their normal design lives. When cracks are discovered in inspection the components must be either repaired or replaced. In most instances it is not economically feasible to replace entire components. Therefore, repairing the damaged areas is both preferred and critical. Additionally, repairs must be made quickly so the aircraft may be returned to service as soon as possible. Also, it is important to be able to model and predict fatigue crack growth behavior (exposed to various spectrum loading situations) that were not accounted for when determining a component's design life.

14. SUBJECT TERMS
AFGROW, fatigue crack prediction code, aging aircraft, repair, adhesive bonding, metallic aircraft structure, widespread fatigue damage, stress level effects, load sequence effects, crack growth

15. NUMBER OF PAGES
44

16. PRICE CODE

17. SECURITY CLASSIFICATION OF REPORT UNCLASSIFIED	18. SECURITY CLASSIFICATION OF THIS PAGE UNCLASSIFIED	19. SECURITY CLASSIFICATION OF ABSTRACT UNCLASSIFIED	20. LIMITATION OF ABSTRACT UL

TABLE OF CONTENTS

LIST OF FIGURES

LIST OF TABLES

FOREWORD

This report was prepared by Analytical Services & Materials, Inc., Hampton Virginia for WL/FIBE, Wright-Patterson Air Force Base, Ohio under contract F33615-94-D-3212, "Structural Integrity Analysis and Verification for Aircraft Structures." The contract program manager was Lt. Dave Conley, WL/FIBE. The government project engineer was James A. Harter. The period of performance for this report was 1 Apr 96 through 31 March 97.

The work performed under this project (Delivery Order 0007) was performed by Analytical Services & Materials, Inc. personnel located at the WL/FIBE Fatigue & Fracture Test Facility, Bldg. 65, Area B, Wright-Patterson AFB, OH. Mr. Kevin L. Boyd was the Principal Investigator of this research. Mr. John H. Elsner and Mr. Kevin L. Boyd authored this report. Mr. Daniel A. McCray and Mr. James A. Harter submitted technical inputs.

1. INTRODUCTION

The purpose of this research is to verify methodologies for AFGROW developed in conjunction with delivery order 0006 [1]. The methodologies, which pertain to aging aircraft, include bonded repair of metallic structures, multiple cracks, stress level effects on crack growth and load sequence effects on crack growth. AFGROW is a fatigue crack growth prediction code developed by AS&M and the Air Force.

This research in necessitated by the growing need to keep current aircraft in service well beyond their normal design lives. When cracks are discovered during inspections the components must be either repaired or replaced. In most instances, it is not economically feasible to replace entire components. Therefore, repairing the damaged areas is both preferred and critical. Additionally, repairs must be made quickly so the aircraft may be returned to service as soon as possible. Also, it is important to be able to model and predict fatigue crack growth behavior (exposed to various spectrum loading situations) that were not accounted for when determining a component's original design life.

2. VERIFICATION TESTING

All verification testing was performed in the Fatigue and Fracture Test Facility, Bldg. 65, Area B, WPAFB, OH. Five servo-hydraulic fatigue test frames were used to test the specimens. The test frames were operated in load control with MTS 458 test controllers at frequencies of 6-10 Hz. Sinusoidal load control signals were generated with MS-DOS based computers running MATE test control software [2]. All testing was completed in an environmental chamber with the relative humidity less than 15%. An air pump was connected to a canister of desiccant, and the air was pumped into a chamber enclosing the middle portion of the specimen. A hygrometer was enclosed in the chamber and when the humidity level in the chamber exceeded 15% the desiccant was replaced and recharged.

2.1 Verification of Repair Analysis Methods

Twelve aluminum 7075-T73 panels of dimensions 16 x 3.95 x 0.086 inches with an EDM center notch of 0.01 x 0.10 inches were precracked at 3.5 kips in RH <15%. After precracking, the specimens were sent to the Wright Lab Materials Directorate where boron epoxy composite patches were applied. A grit blast/silane surface preparation was used on all panels [3]. Since the patches were only 7 plies, only slight sanding was used for surface preparation for 10 of the patches. The other two specimens (007-1-06 and 007-1-10) were grit blasted. The 1.8 x 5.6 inch patches were centered on the specimen and bonded to the panels with FM-73, AF 163-2 or EA 9394 adhesive.

The following is a brief summary of the adhesives. FM 73 is a film adhesive manufactured by Cytec and was cured at 250°F for 1 hour at 35 psi. AF 163-2 is a film adhesive manufactured by 3M and was cured at 250°F for 1 hour at 35 psi. Since aluminum has a higher coefficient of thermal expansion, the curing process leaves thermal residual stresses in the panel and patch after cooling to room temperature. The residual stresses were obvious due to the noticeable curvature in the specimens. EA 9394 is a paste adhesive manufactured by Dexter-Hysol that can be used as either an elevated or room temperature cure adhesive. For this study, the paste was allowed to harden overnight under pressure at room temperature, then subjected to 200°F for 1 hour to fully cure the adhesive. Minimal thermal residual stresses are expected with this procedure.

A schematic of the specimens can be seen in Figure 1. Two of the specimens had five strain gages applied at locations noted in Figure 1. The patched specimens were then subjected to three different analysis-testing combinations. All specimens were cyclically constant amplitude tested with a maximum load of 6.265 kips and a load ratio of 0.05. Table 1 contains the analysis-testing combinations: eight specimens were C-scanned at periodic crack length and cycled until failure, two specimens were C-scanned at periodic crack lengths and residual strength tested once the crack reached the edge of the patch. The remaining two specimens with strain gages were strain-analyzed at periodic crack

lengths. These specimens were loaded to 6 kips in 10 seconds, held at 6 kips for 4 seconds, then released for 10 seconds in order to obtain a strain profile for the five locations listed in Figure 1. The specimens were then cycled until failure. The data for all specimens including crack length at analysis, lifetimes and residual strengths are listed in Table 2- Table 4.
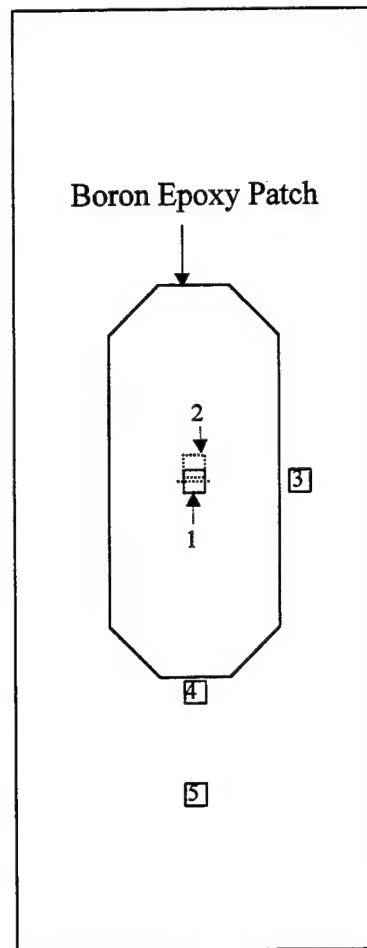
Figure 1: Schematic of aluminum specimen with boron epoxy patch.

(The number represent strain gages labeled as 1) patch, 2) skin, 3) by-pass, 4) near, 5) remote.)

Table 1: List of test types and number of specimens with adhesive types for boron epoxy patch bonded to aluminum 7075-T73.

Analysis - Test type	Number of specimens	Adhesive
C-scan – Life	8	(2) FM 73, (2) AF 163-2, (4) EA 9394
C-scan – Residual strength	2	FM-73, AF 163-2
Strain survey - Life	2	FM-73, AF 163-2

Table 2: List of C-scan-life tested bonded composite specimens.

Specimen	Frame	Adhesive	C-scan		Cycles to Failure
			cycles	a (inches)	
007-1-01	15	FM-73	0	0.117	72,774
			35,004	0.443	
			48,150	0.708	
			61,210	1.011	
			66,538	1.227	
007-1-02	15	EA 9394	0	0.120	101,536
			53,538	0.419	
			75,078	0.717	
			87,096	0.998	
007-1-04	15	FM-73	0	0.117	66,341
			31,647	0.405	
			47,491	0.715	
			56,812	1.015	
007-1-06	14	EA 9394	0	0.117	81,885
			41,568	0.418	
			58,069	0.724	
			68,640	0.999	
007-1-09	14	EA 9394	0	0.116	104,068
			56,042	0.417	
			77,587	0.718	
			89,615	1.002	
007-1-10	15	EA 9394	0	0.117	75,332
			39,495	0.438	
			54,070	0.723	
			64,097	1.019	
007-1-11	14	AF 163-2	0	0.118	69,662
			30,004	0.402	
			44,457	0.678	
			57,706	0.967	
			63,543	1.205	
007-1-12	14	AF 163-2	0	0.116	69,477
			31,648	0.404	
			49,796	0.716	
			59,124	1.004	

4

Table 3: List of C-scan - residual strengths of bonded composite specimens.
(Residual strength test at maximum crack length in table.)

Specimen	Frame	Adhesive	C-scan		Residual strength
			cycles	a (inches)	
007-1-05	14	FM-73	0	0.115	18.5 kips
			40,003	0.354	
			58,006	0.667	
			68,865	0.966	
			70,074	1.010	
007-1-07	15	AF 163-2	0	0.117	19.0 kips
			40,002	0.565	
			45,006	0.679	
			53,552	0.905	
			55,565	0.978	

Table 4: List of strain analysis – life tested bonded composite specimens.

Specimen	Frame	Adhesive	Strain Survey		Cycles to Failure
			cycles	a (inches)	
007-1-03	14	FM-73	0	0.118	67,726
			33,046	0.429	
			50,073	0.728	
			55,686	0.952	
007-1-08	14	AF 163-2	0	0.119	61,088
			28,570	0.421	
			42,111	0.720	
			50,641	0.985	
			60,184	1.506	

Crack length versus cycle count data was recorded and plotted for all specimens. Figure 2 - Figure 13 are plots of crack lengths versus cycles for all specimens. Specimens 007-1-05 and 007-1-07 (Figure 6 and Figure 8, respectively) were residual strength tested after the crack reached the edge of the patch. The adhesives for these two specimens were FM-73 and AF 163-2, respectively, and the residual strengths were nearly identical. Both specimens failed at the adhesive–patch interface, suggesting that the bond between the adhesive and patch was inadequate. The rest of the specimens were fatigue tested until failure.

The three specimens with FM-73 adhesive were compared to AFGROW predictions. AFGROW v3.82.1 was used for the predictions, and the adhesive database consists of only FM-73. Some of the information needed to use the repair module in AFGROW include patch material, orientation, number of plies, cure temperature, bending

allowance, and disbond ratio (0.29 disbond ratio was used measured from C-scan). The cure temperature and bending allowance were varied during AFGROW analysis. The effect of the residual stresses resulting from high temperature curing is entered as ΔT, which is the difference between the cure temperature and room temperature. The bending allowance has a check-off box, either bending from a single side patch is allowed or it is not.

Modeling the testing conditions is difficult because the stresses are complex. The specimens with FM-73 adhesive are curved from the thermal residual stresses, but gripping the specimen lessens the curvature. When the specimen is axially loaded, bending from a single sided patch will counter the curvature from the residual thermal stresses, and an undetermined amount of loading is required to overcome the compressive residual stress. The load required to overcome the residual thermal stresses (or curvature) can be modeled as a negative ΔT. A negative ΔT imparts a compressive residual stress whereas a positive ΔT imparts a tensile residual stress. Since the panel is in compression after curing (from bending), a negative ΔT seems to be a reasonable modeling technique. Three conditions were used with the AFGROW predictions. The first one allows bending with $\Delta T=0$, and the prediction is conservative. The second condition allows bending with $\Delta T=-25$, and the prediction is less conservative. Using $\Delta T=-25$ is the more accurate representation because positive loading is needed to overcome the residual thermal stresses. The negative ΔT will emulate this situation. The third condition did not allow bending with $\Delta T=50$, and the prediction was very accurate for all three specimens. Although the no-bending situation with $\Delta T=50$ is not very representative, something can be learned from it. According to the predictions, the bending correction seems to be too aggressive due to the shape of the curves. The bending correction solution with $\Delta T=0$ seems to track the data until a=0.5 inches. After a=0.5 inches, the bending correction becomes too aggressive. One possible explanation is that bending diminishes as the crack length increases.
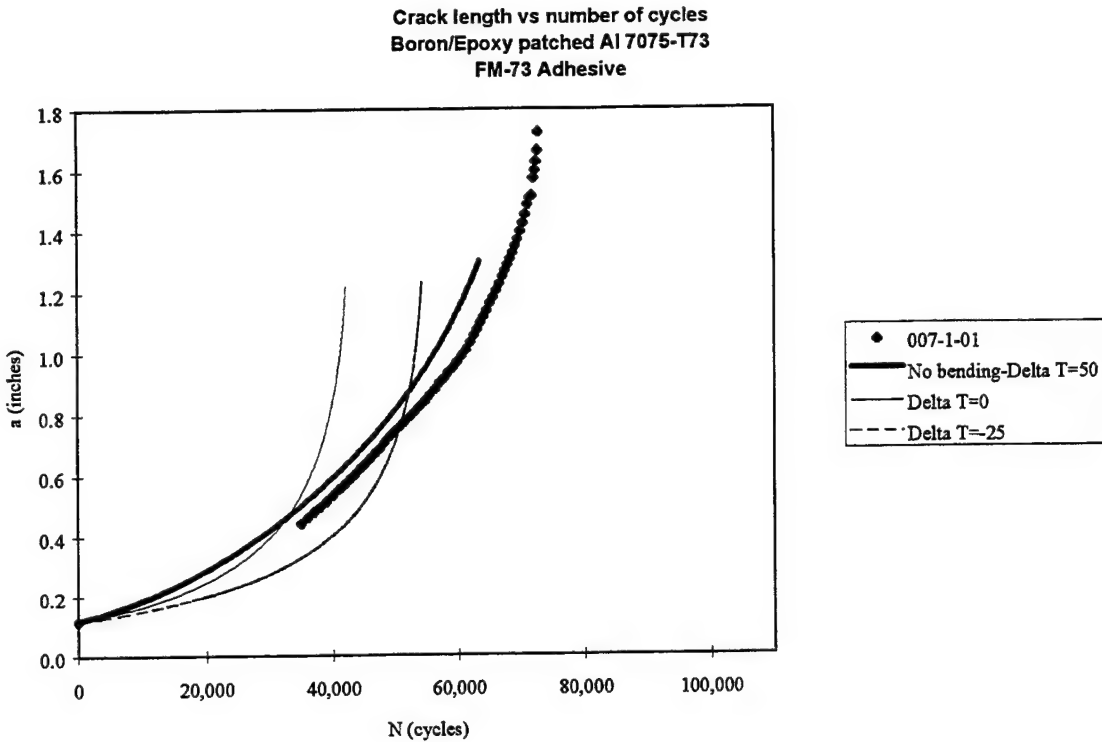
6

Crack length vs number of cycles
Boron/Epoxy patched Al 7075-T73
FM-73 Adhesive

Figure 2: Crack growth curve and AFGROW predictions for specimen 007-1-01 with FM – 73 adhesive.

Crack length vs number of cycles
Boron/Epoxy patched Al 7075-T73
EA 9394 Adhesive
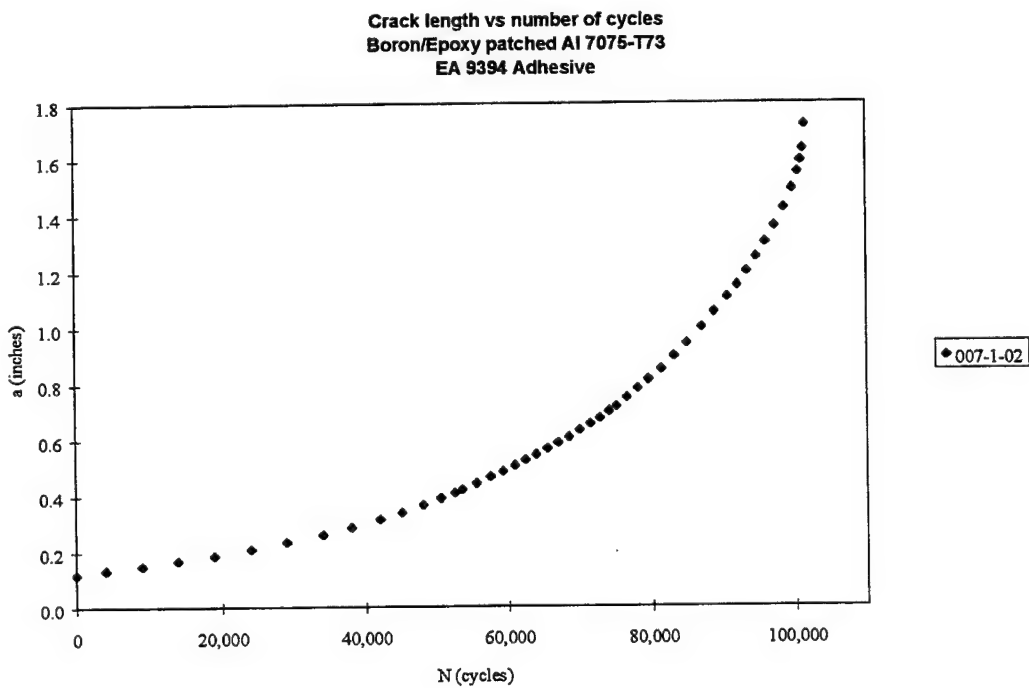
Figure 3: Crack growth curve for specimen 007-1-02 with EA 9394 adhesive.

7

Crack length vs number of cycles
Boron/Epoxy patched Al 7075-T73
FM - 73 Adhesive
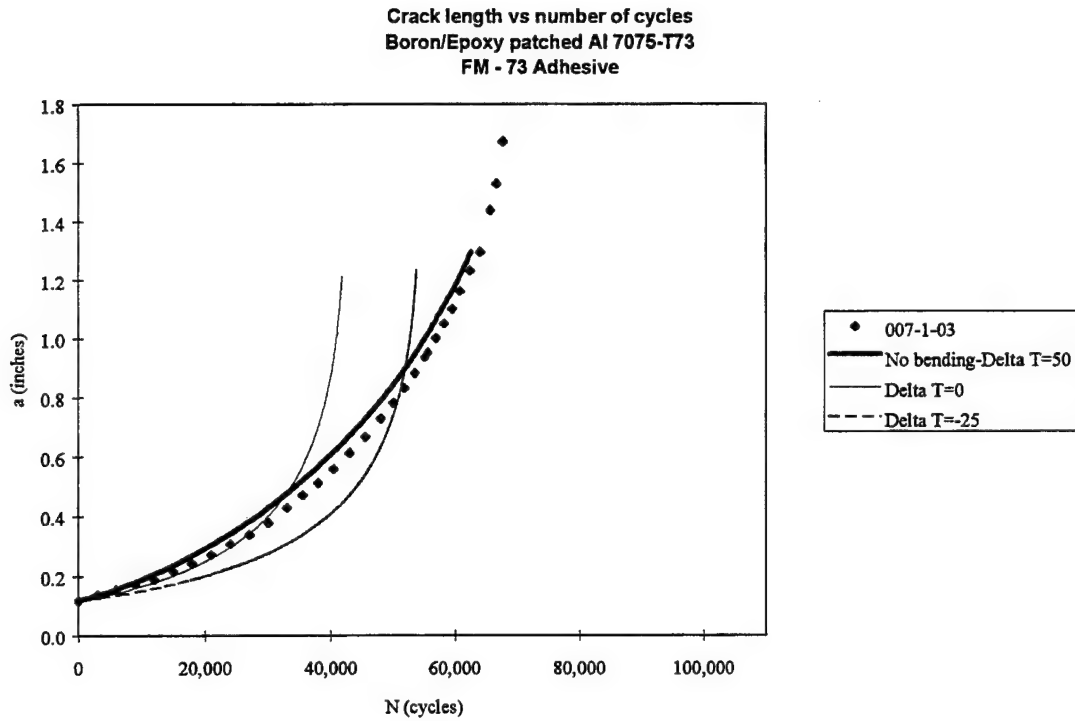
Figure 4: Crack growth curve and AFGROW predictions for specimen 007-1-03 with FM - 73 adhesive.

Crack length vs number of cycles
Boron/Epoxy patched Al 7075-T73
FM - 73 Adhesive
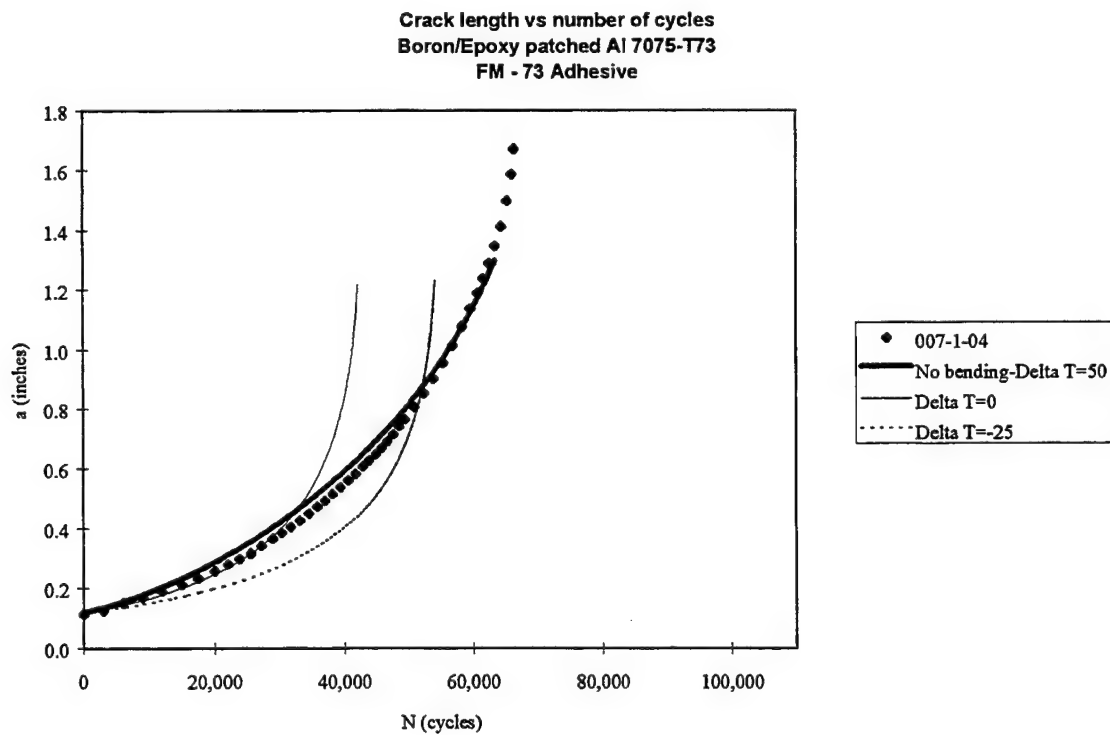
Figure 5: Crack growth curve and AFGROW predictions for specimen 007-1-04 with FM – 73 adhesive.

8

Crack length vs number of cycles
Boron/Epoxy patched Al 7075-T73
FM-73 Adhesive

007-1-05
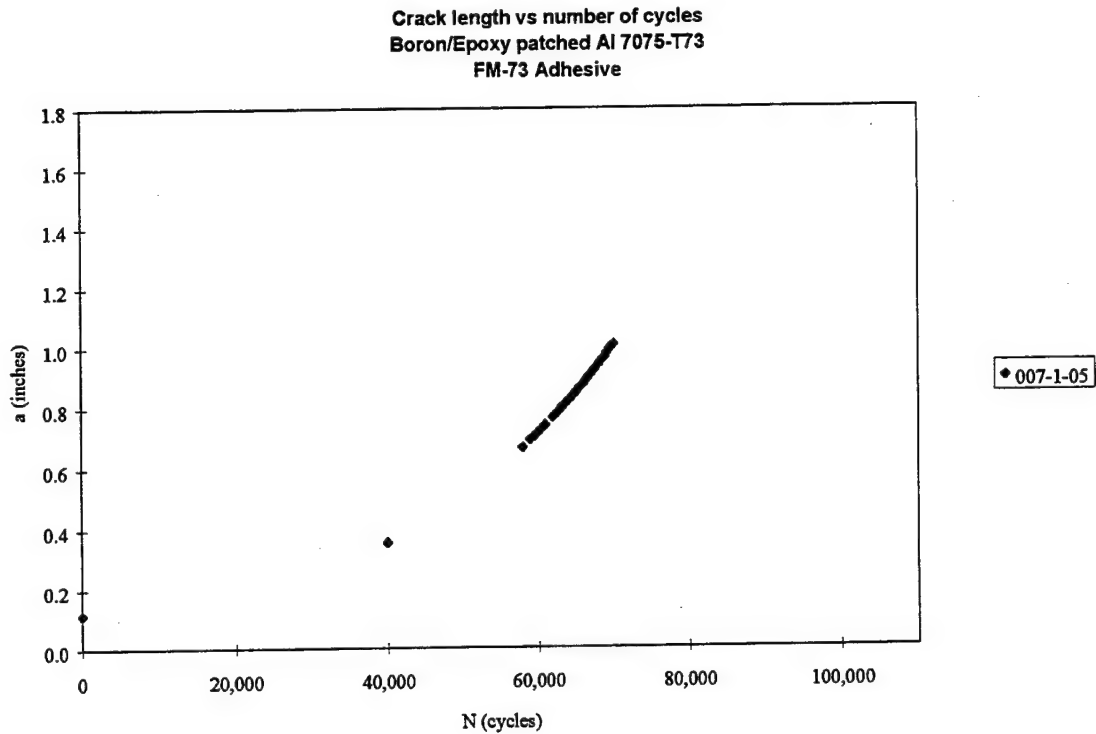
Figure 6: Crack growth curve for specimen 007-1-05 with FM – 73 adhesive.
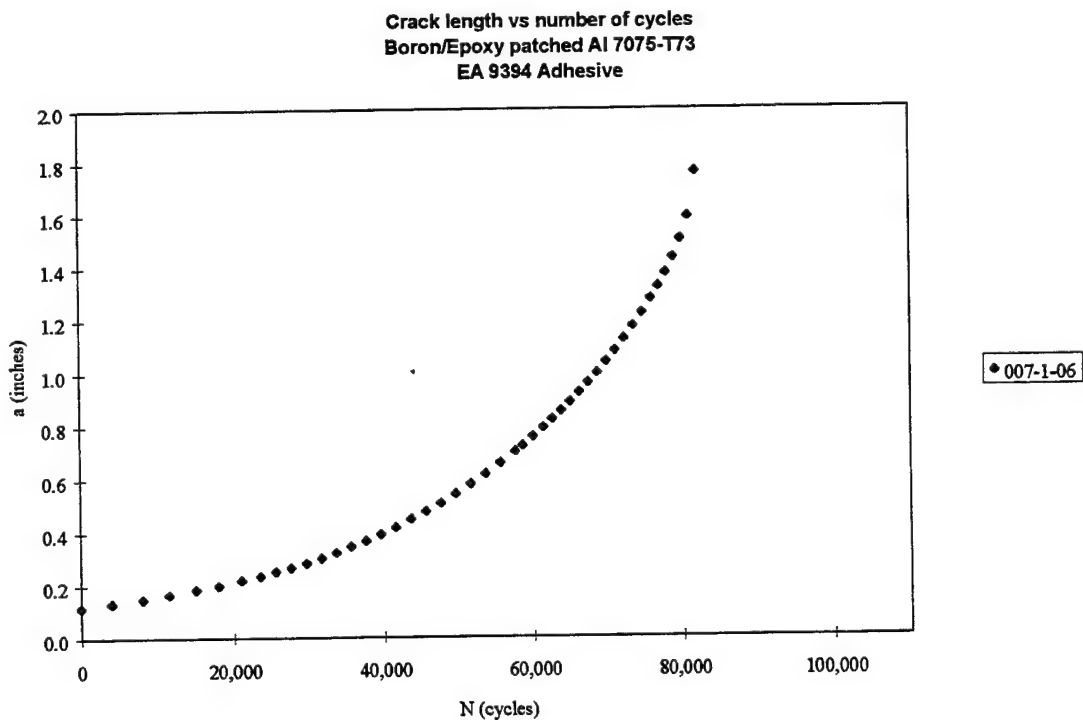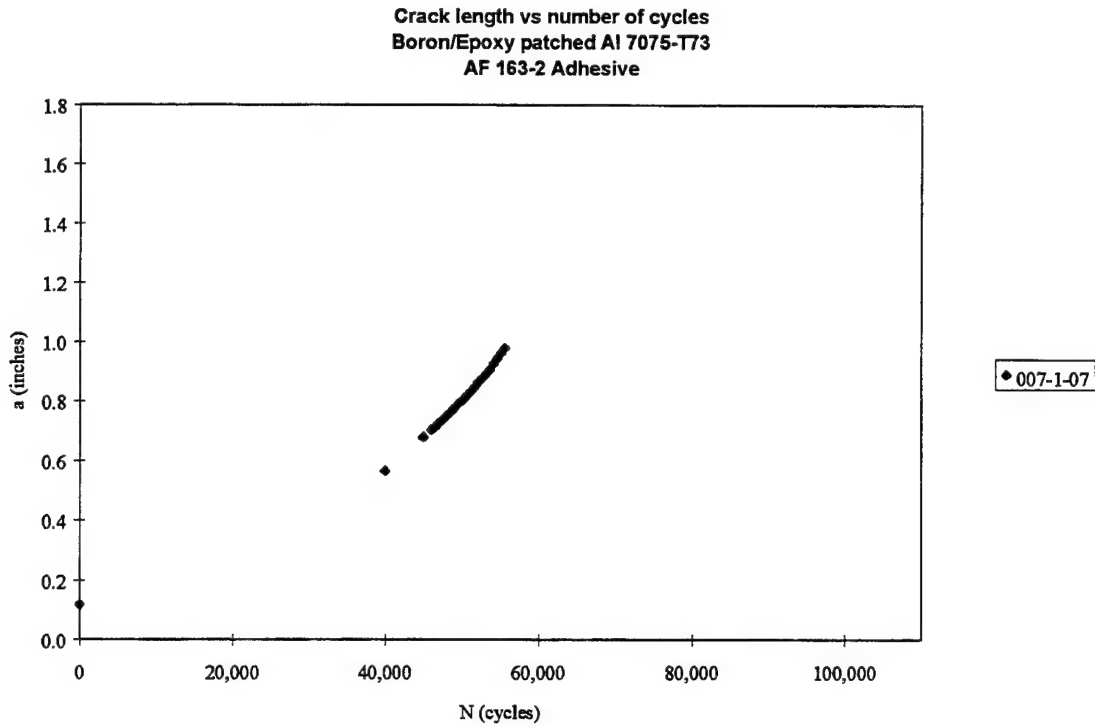(The specimen was residual strength tested.)

Crack length vs number of cycles
Boron/Epoxy patched Al 7075-T73
EA 9394 Adhesive

007-1-06

Figure 7: Crack growth curve for specimen 007-1-06 with EA 9394 adhesive.

9

Crack length vs number of cycles
Boron/Epoxy patched Al 7075-T73
AF 163-2 Adhesive

Figure 8: Crack growth curve for specimen 007-1-07 with AF 163–2 adhesive.
(The specimen was residual strength tested.)

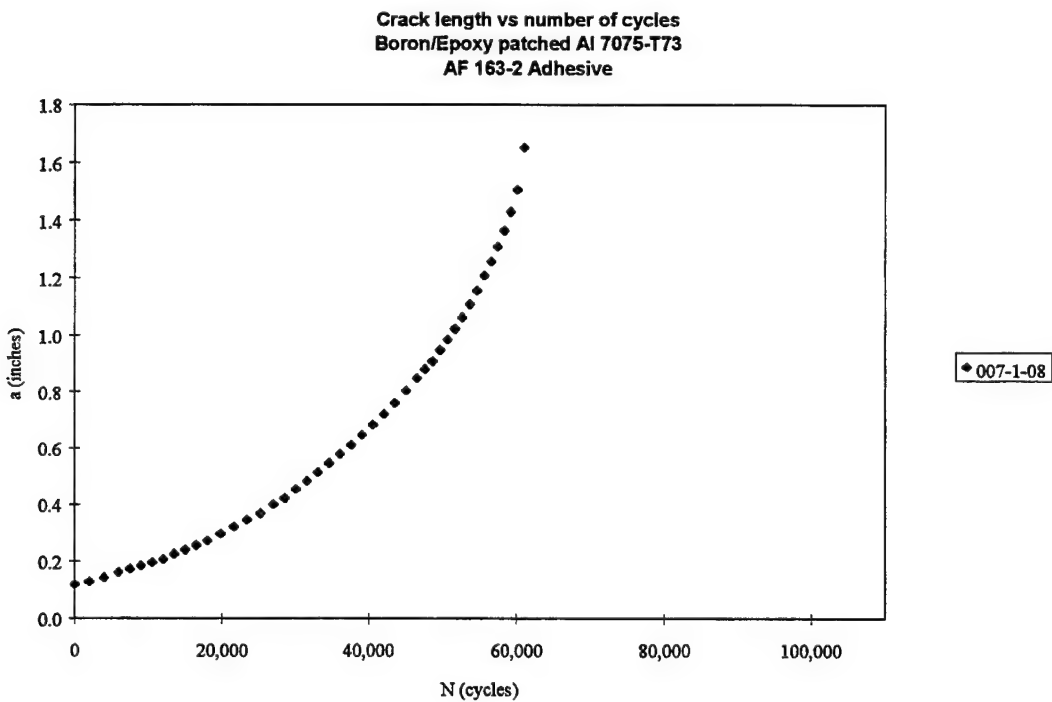**Crack length vs number of cycles**
Boron/Epoxy patched Al 7075-T73
AF 163-2 Adhesive

Figure 9: Crack growth curve for specimen 007-1-08 with AF 163–2 adhesive.

10

Crack length vs number of cycles
Boron/Epoxy patched Al 7075-T73
EA 9394 Adhesive
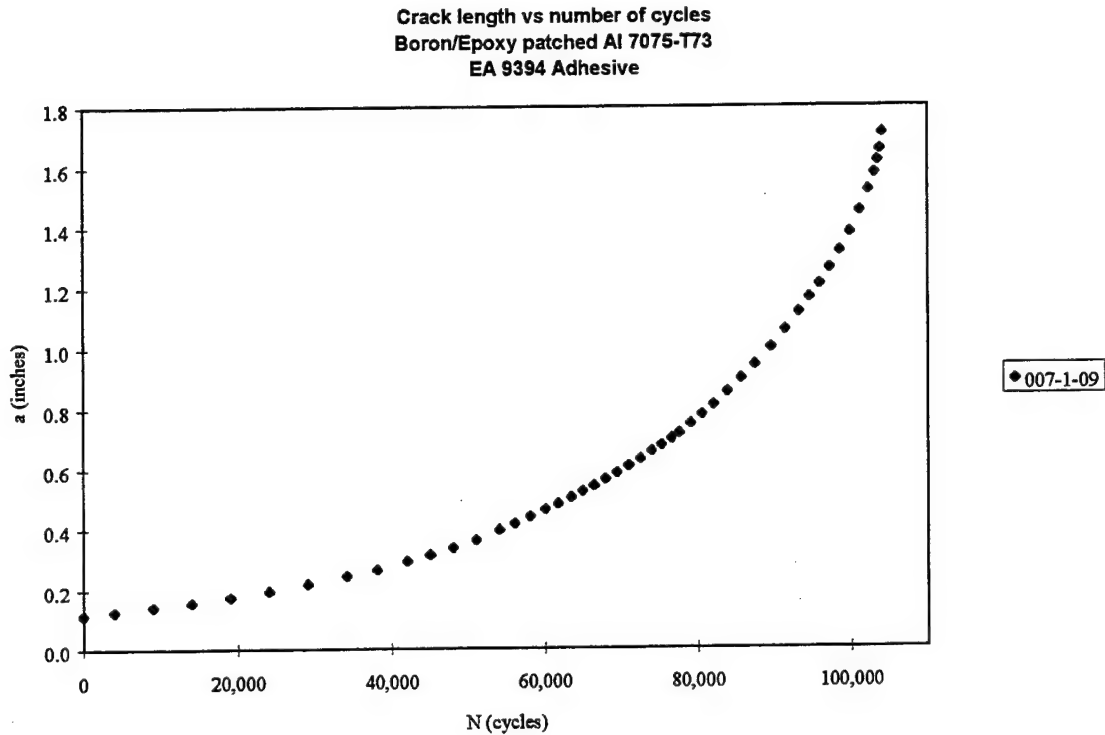
Figure 10: Crack growth curve for specimen 007-1-09 with EA 9394 adhesive.

Crack length vs number of cycles
Boron/Epoxy patched Al 7075-T73
EA 9394 Adhesive
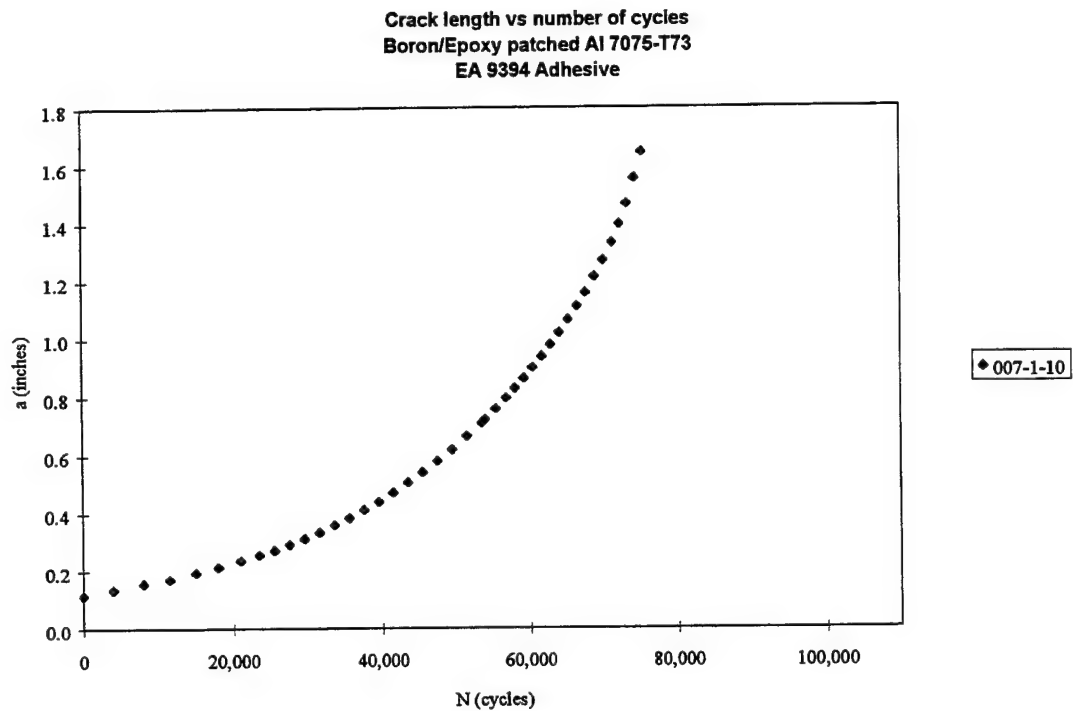
Figure 11: Crack growth curve for specimen 007-1-10 with EA 9394 adhesive.

11

Crack length vs number of cycles
Boron/Epoxy patched Al 7075-T73
AF 163-2 Adhesive
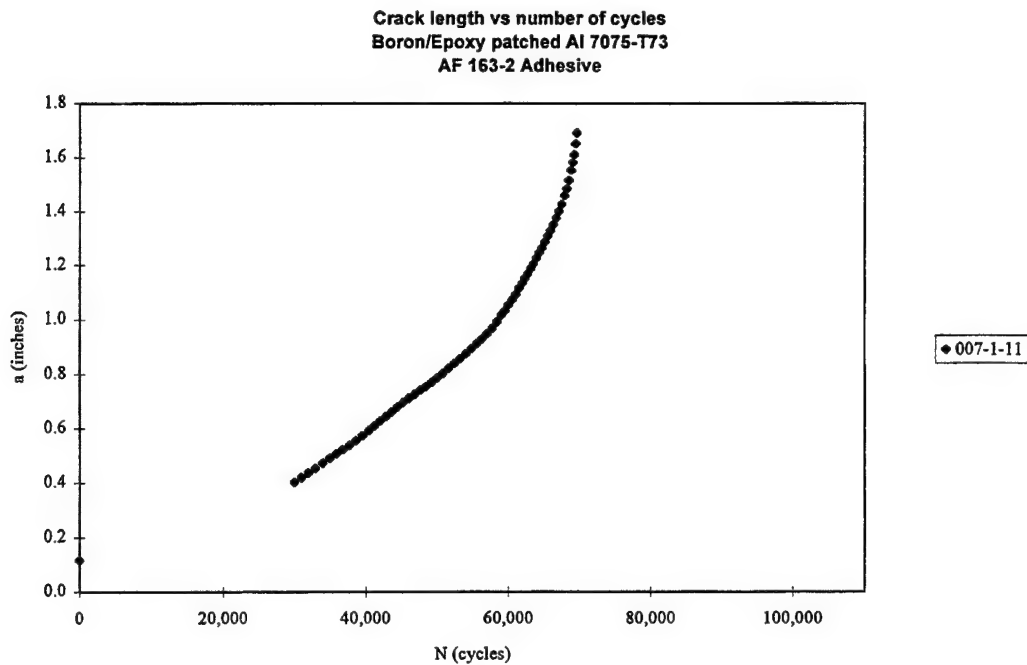
Figure 12: Crack growth curve for specimen 007-1-11 with AF 163-2 adhesive.

Crack length vs number of cycles
Boron/Epoxy patched Al 7075-T73
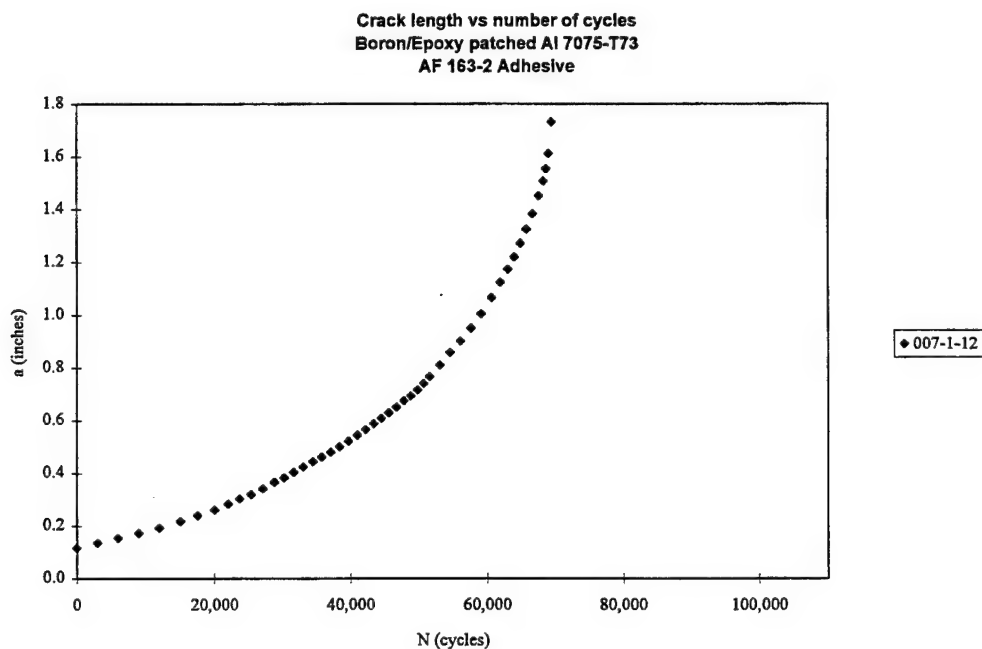**AF 163-2 Adhesive**

Figure 13: Crack growth curve for specimen 007-1-12 with AF 163 -2 adhesive.

Ten specimens were C-scanned to determine the amount of debonding during crack growth. C-scanning transmits energy through the aluminum panel and composite patch.

12

The better the bond between the panel and patch, the greater the amount of energy that will be transmitted and recorded by the C-scan. So as the fatigue crack grows under the patch, the aluminum and patch disbond from each other and can be visualized by the lower energy area on the C-scan.

Figure 14 shows the growth of the debonded area of specimen 007-1-01. The C-scans of the other nine specimens are shown in Figure 15. The C-scans were taken when the crack was at the edge of the patch and correspond to the lower left C-scan in Figure 14.
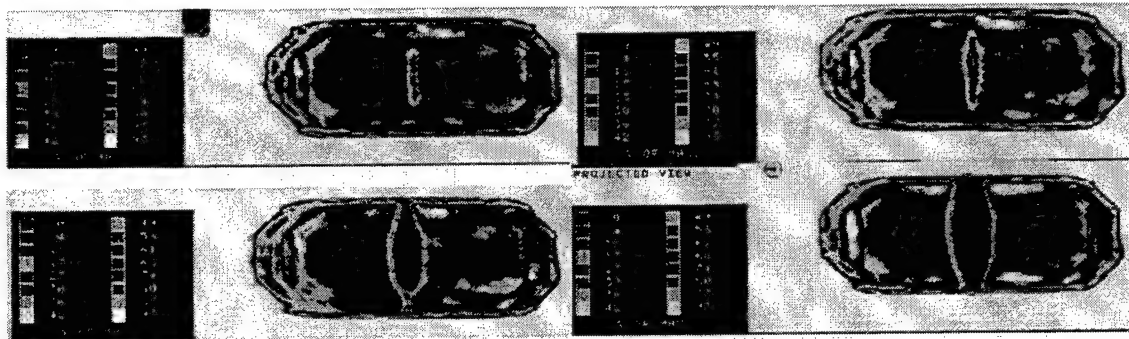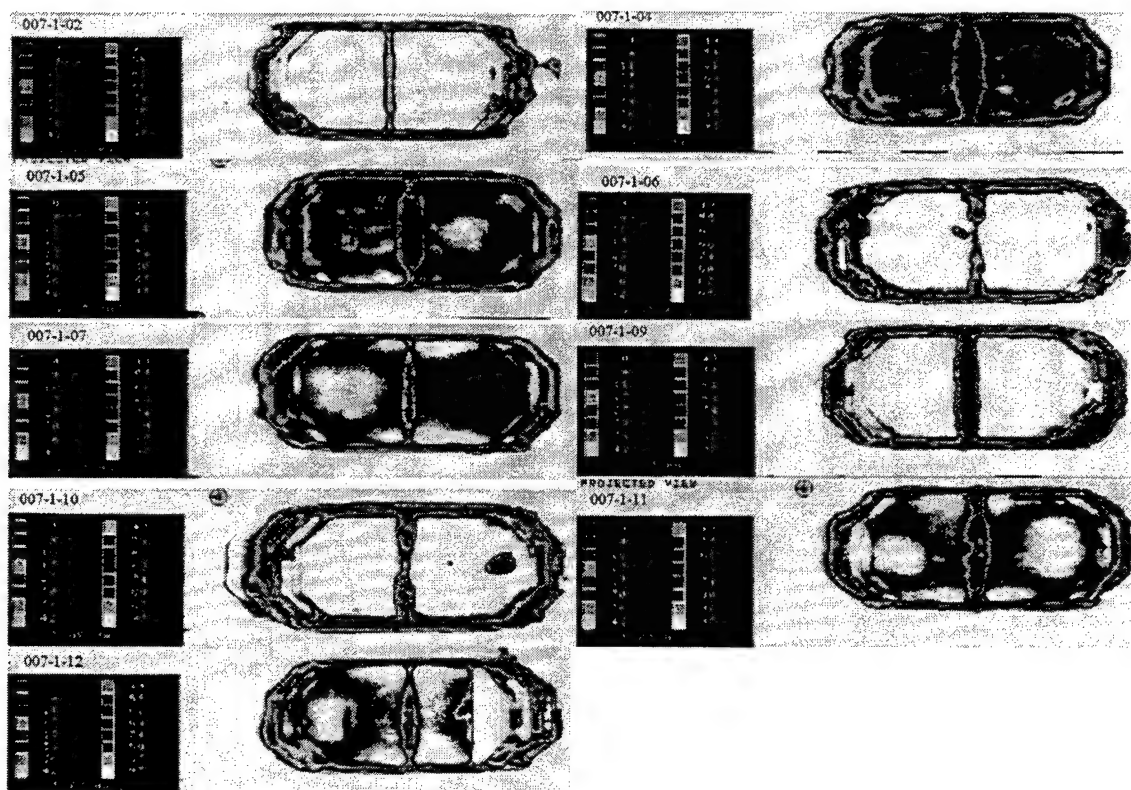

Figure 14: C-scan images of specimen 007-1-01.

(Top left image corresponds to shortest crack length, and crack length versus cycles can be found in Table 2.)

Figure 15: C-scan images of specimens when crack was at the edge of the patch.

(Specimen number located on each C-scan.)

Strain analysis was performed on two specimens. The locations of the strain gages are shown in Figure 1. The specimens were loaded to 6 kips at a frequency of 0.05 Hz with a 4 second hold at the peak. The strain analyses were performed at the same crack increments as the C-scans. Figure 16 - Figure 19 are the strain profiles for specimen 007-1-03, and Figure 20 – Figure 24 are the strain profiles for specimen 007-1-08. The unusual strain readings are from the gage on the patch. Under tensile loading, the strain on the outside of the patch is in compression. The curvature of the specimen causes the compressive strain. With no applied load, the specimen still has a curvature, and once the load is applied, the specimen straightens out. The unbonded patch surface compresses until the patch straightens out, then it will start to become tensile.
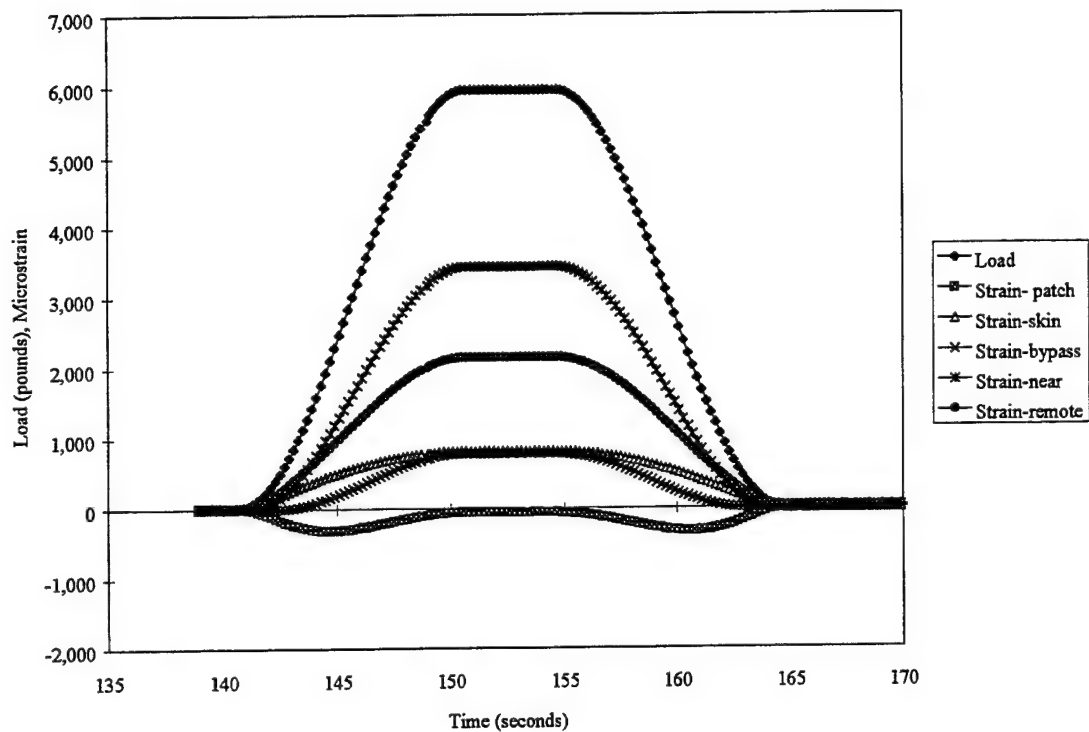
Figure 16: Load and strain data for specimen 007-1-03 with a crack length of a=0.118 inches.
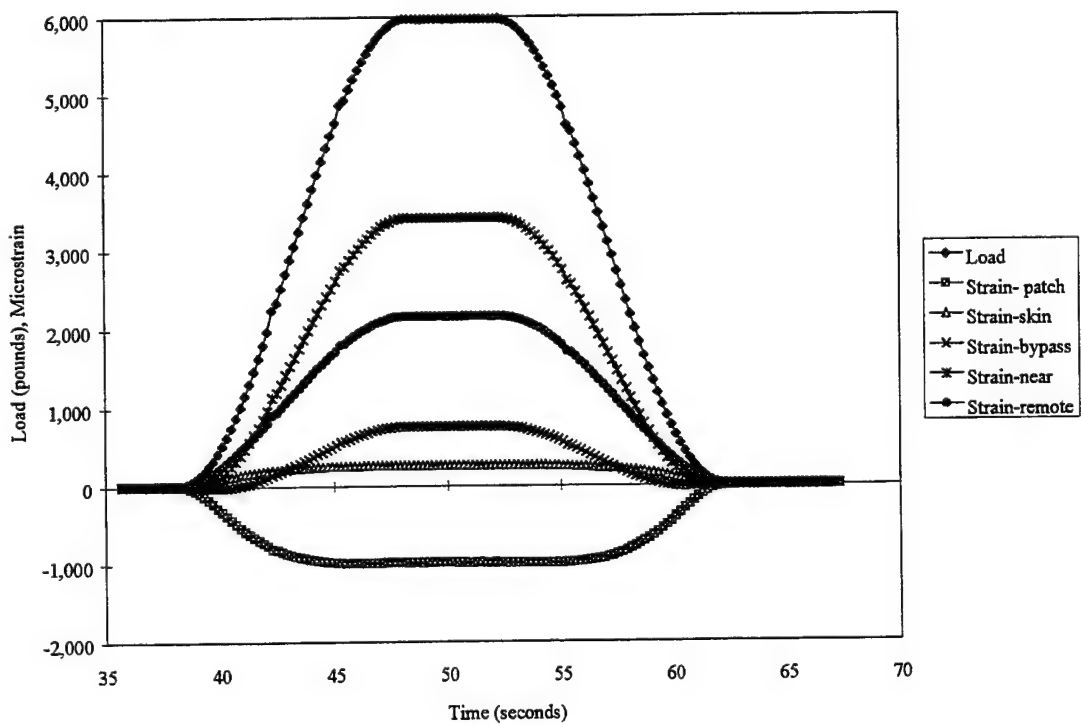

Figure 17: Load and strain data for specimen 007-1-03 with a crack length of a=0.429 inches.
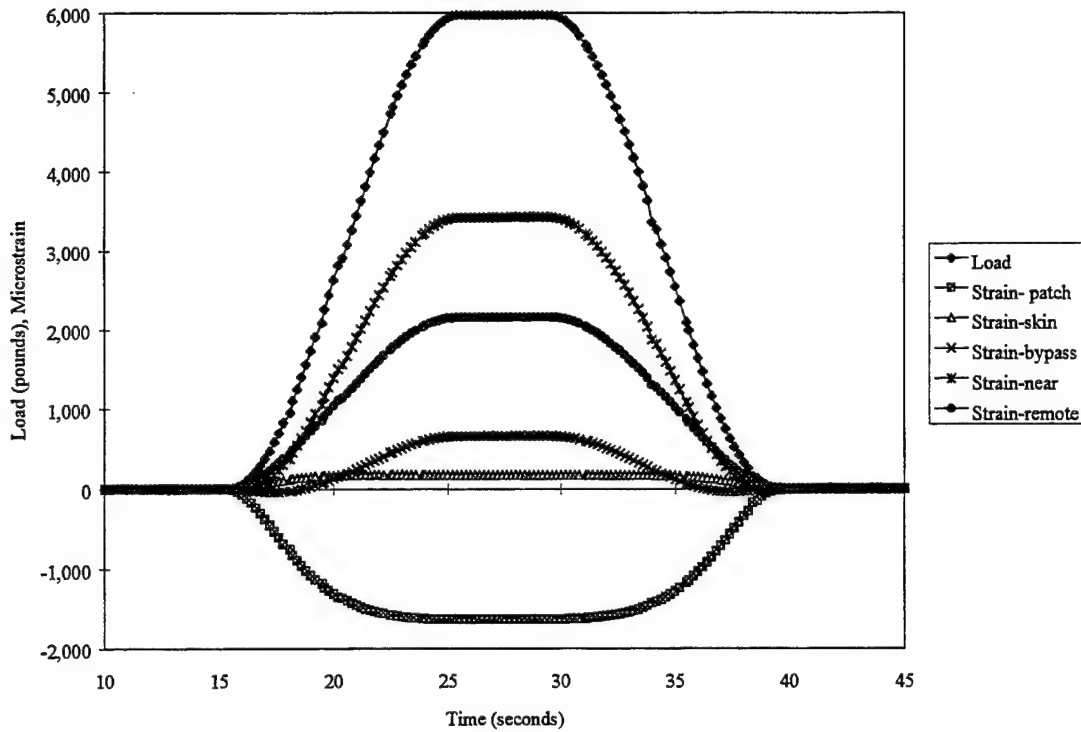
15

Figure 18: Load and strain data for specimen 007-1-03 with a crack length of a=0.728 inches.
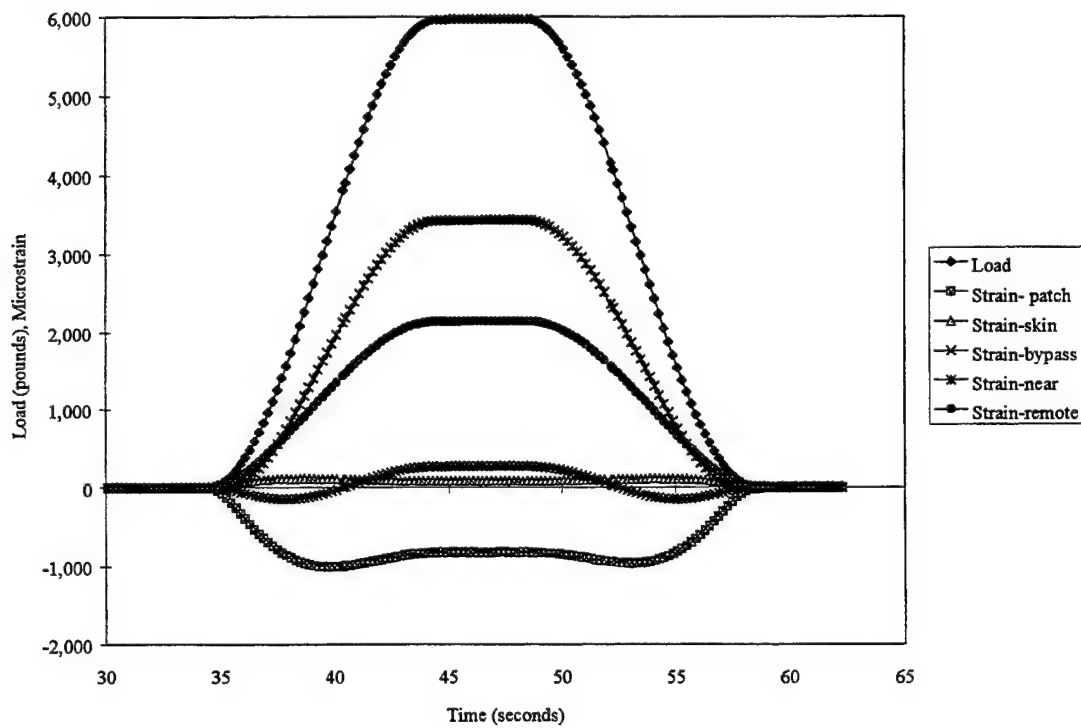

Figure 19: Load and strain data for specimen 007-1-3 with a crack length of a=0.952 inches.
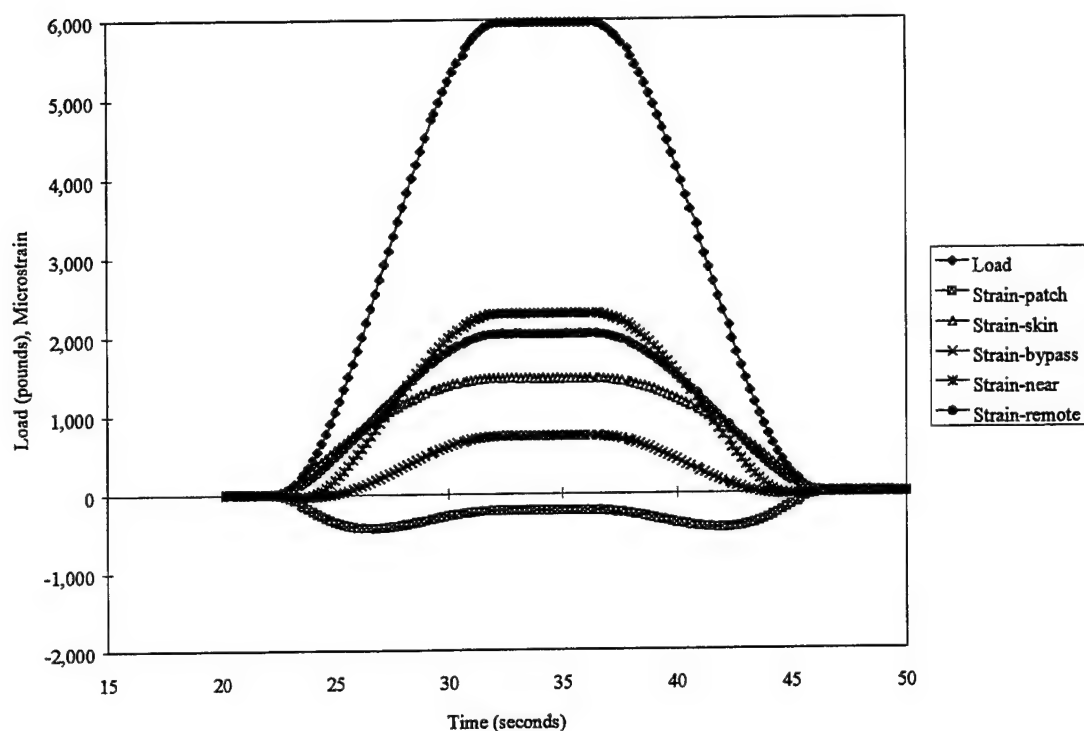
16

Figure 20: Load and strain data for specimen 007-1-08 with a crack length of a=0.119 inches.

Figure 21: Load and strain data for specimen 007-1-08 with a crack length of a=0.421 inches.

17

Figure 22: Load and strain data for specimen 007-1-08 with a crack length of a=0.720 inches.

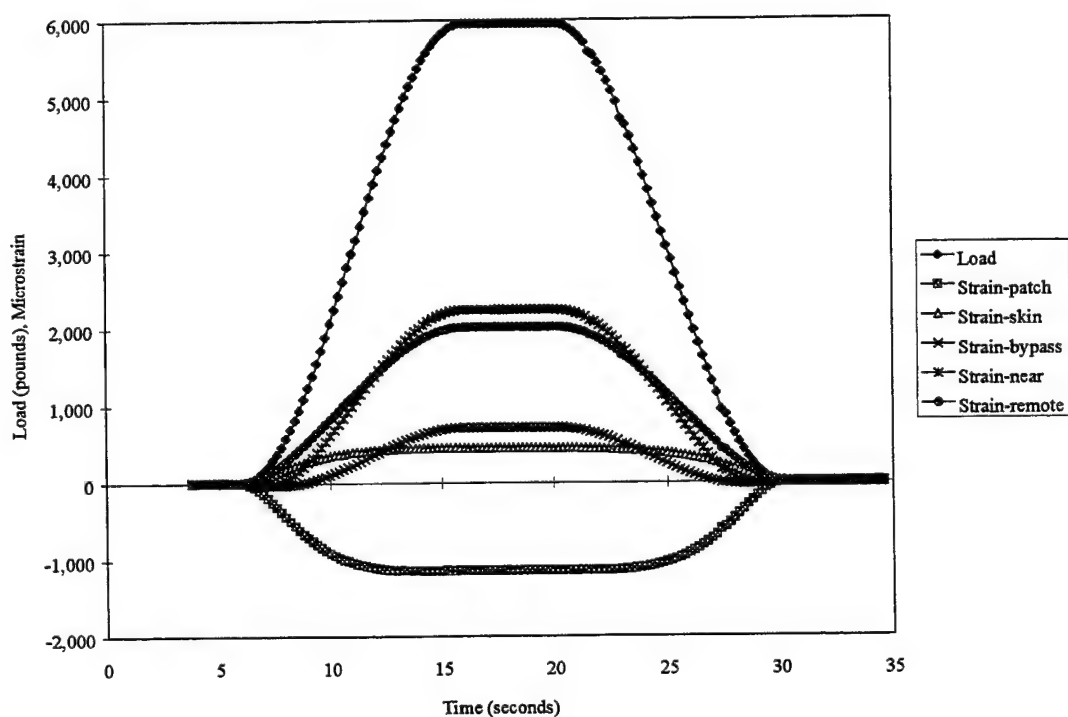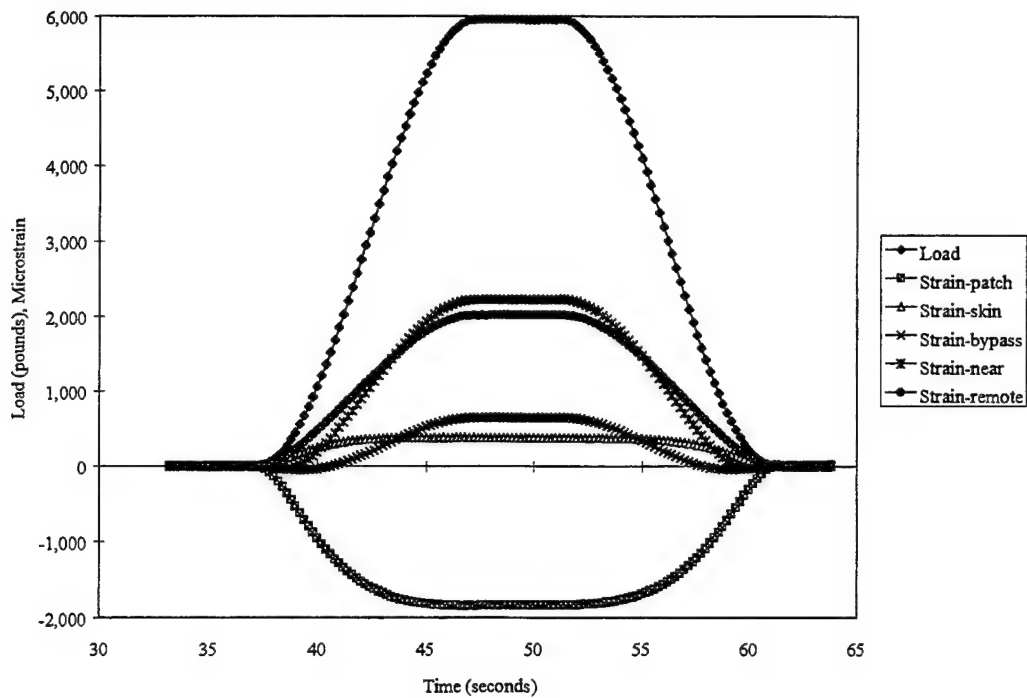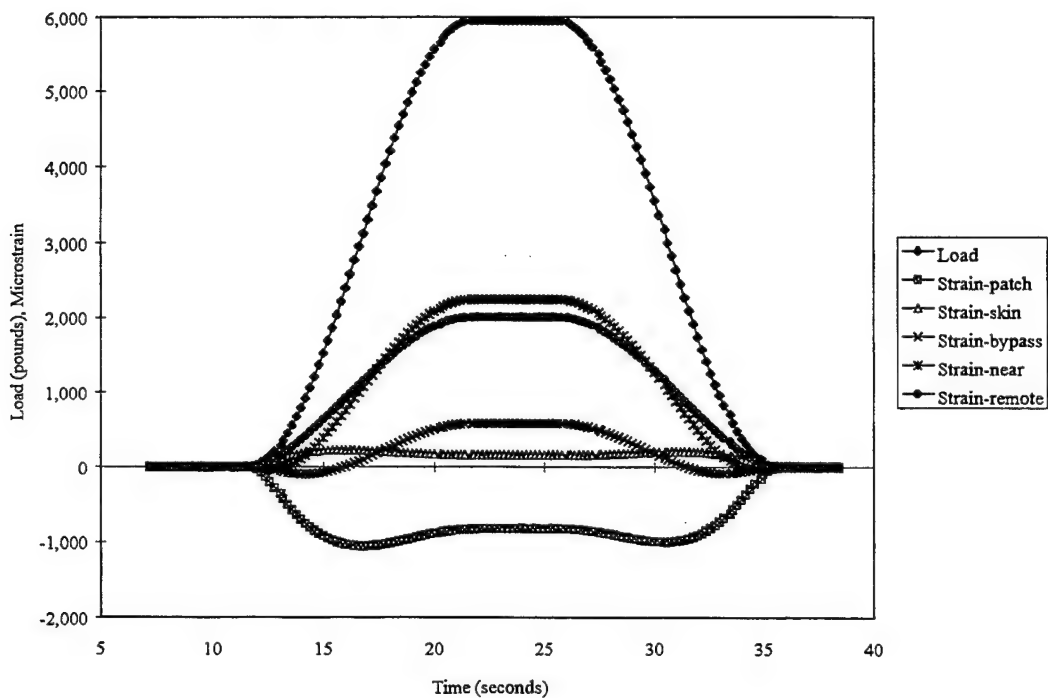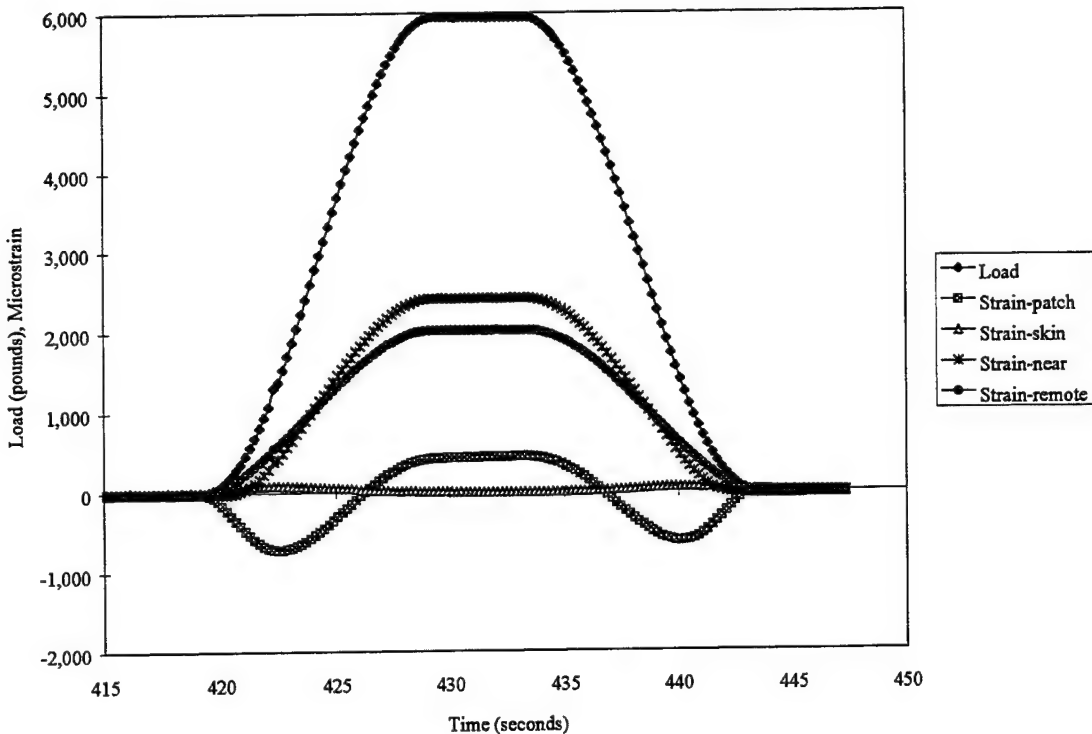**Figure 23: Load and strain data for specimen 007-1-08 with a crack length of a=0.985 inches.**

18

Figure 24: Load and strain data for specimen 007-1-08 with a crack length of a=1.506 inches. (The by-pass strain gage was inoperable)

2.2   Multiple Cracks

The specimens were 16x3.95x0.25 inch panels of 7075-T73 with four different crack configurations shown in Figure 25. The open hole specimens had EDM notches of 0.048 inch for notch "a" in configurations A and D. Notch "a" was 0.058 inch in configuration B and C. Notch "b" was 0.257 inch in configuration B and C, and 0.247 inch in configuration D. The specimens were precracked at a stress ratio of 0 and in RH <15%. The precracking schedule is shown in Table 5. The specimens were then tested under constant amplitude fatigue loading at a maximum load of 5 kips and a stress ratio of 0.1 with RH <15% until specimen failure. Graphs of crack size versus cycles are shown in Figure 26 - Figure 32. Figure 26 is the plot for both of the single crack specimens. AFGROW has the same specimen configuration and AFGROW predictions using RH <15% and lab air data for predictions are also plotted. The data fits well with the RH <15% prediction.
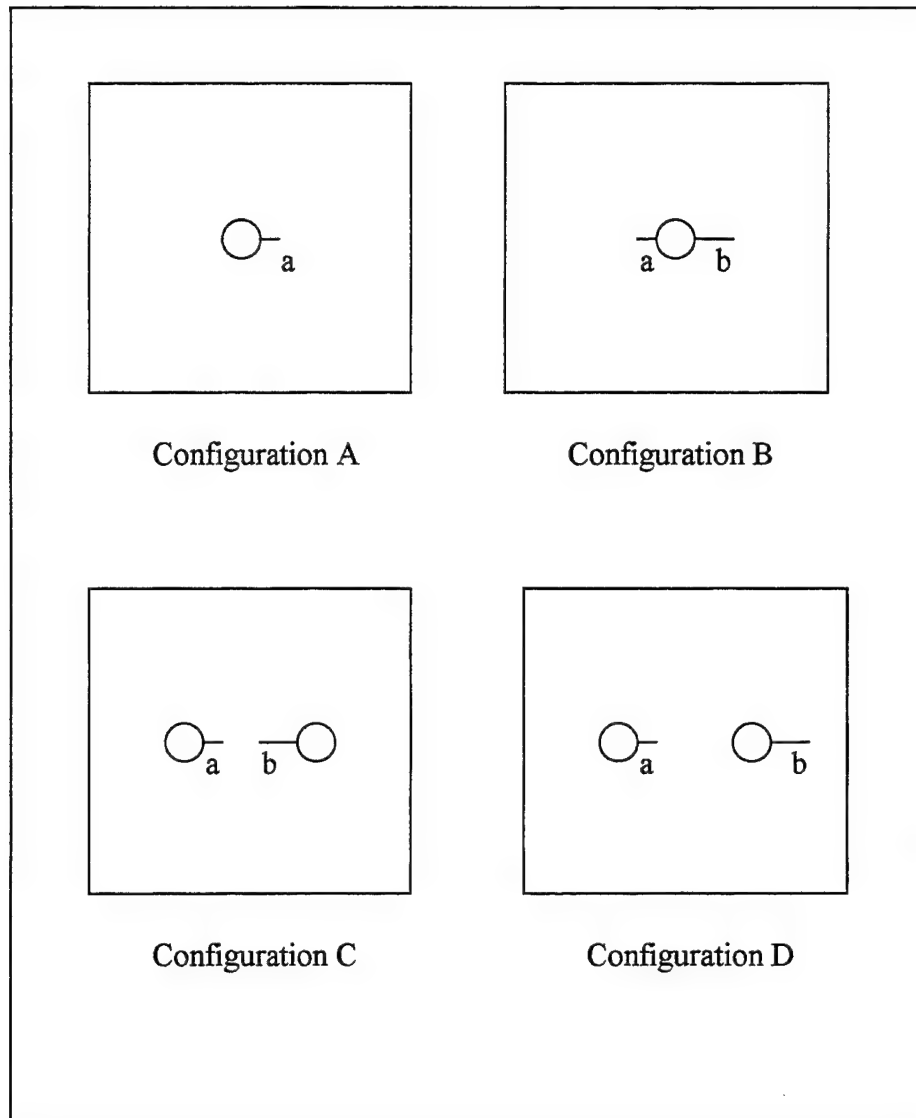
19

Configuration A

Configuration B

Configuration C

Configuration D

Figure 25: Multiple crack specimen configurations.

Table 5: Precracking schedule for multiple crack specimens.

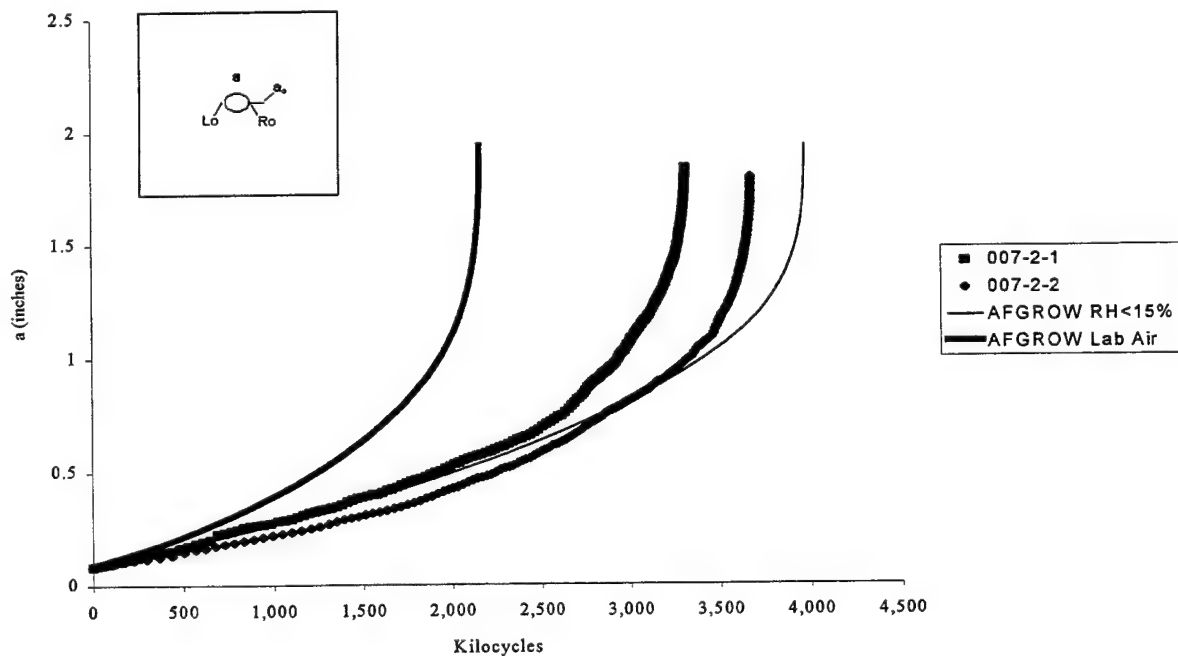| Specimen	Configuration	Max Load (kips)	Crack Extension (inches) a	b
007-2-1	A	10	0.005	x
		8	0.010	x
		6	0.009	x
		4.8	0.010	x
007-2-2	A	10	0.008	x
		8	0.009	x
		6	0.005	x
		4.8	0.011	x
007-2-3	B	5	0.099	0.100
007-2-4	B	5	0.102	0.088
007-2-5	C	5	0.040	0.047
007-2-6	C	5	0.068	0.092
007-2-7	D	5	0.043	0.081
007-2-8	D	5	0.044	0.082

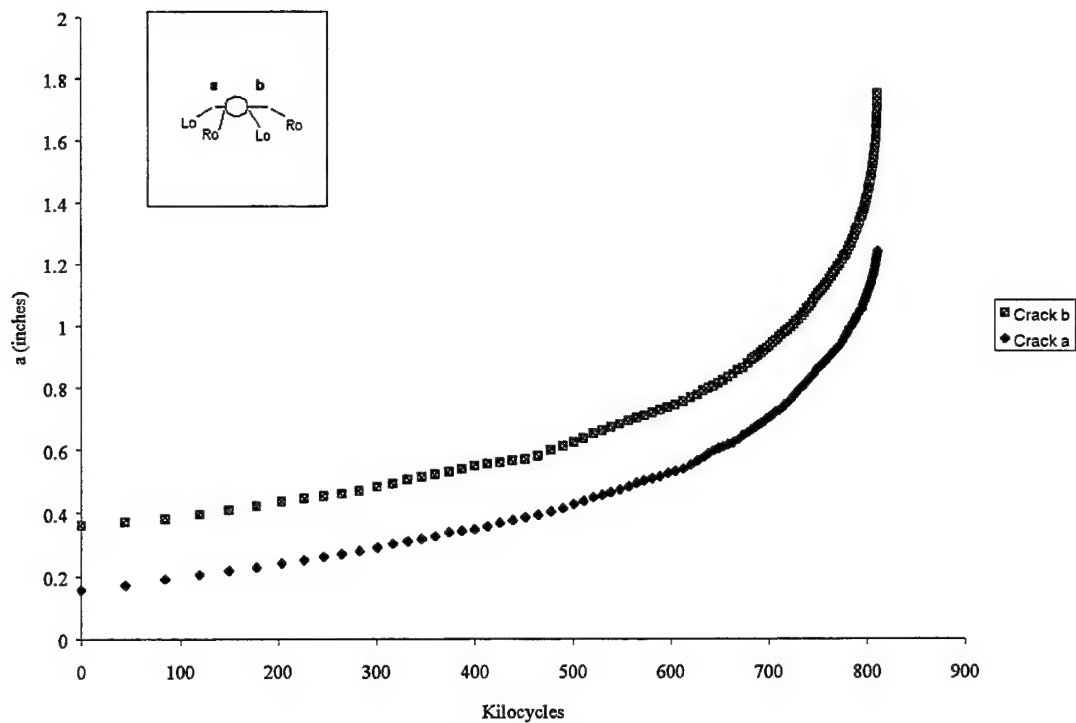**Figure 26: Crack growth data for configuration A specimens, with AFGROW predictions.**

21

Figure 27: Crack growth plot for specimen 007-2-3 configuration B.
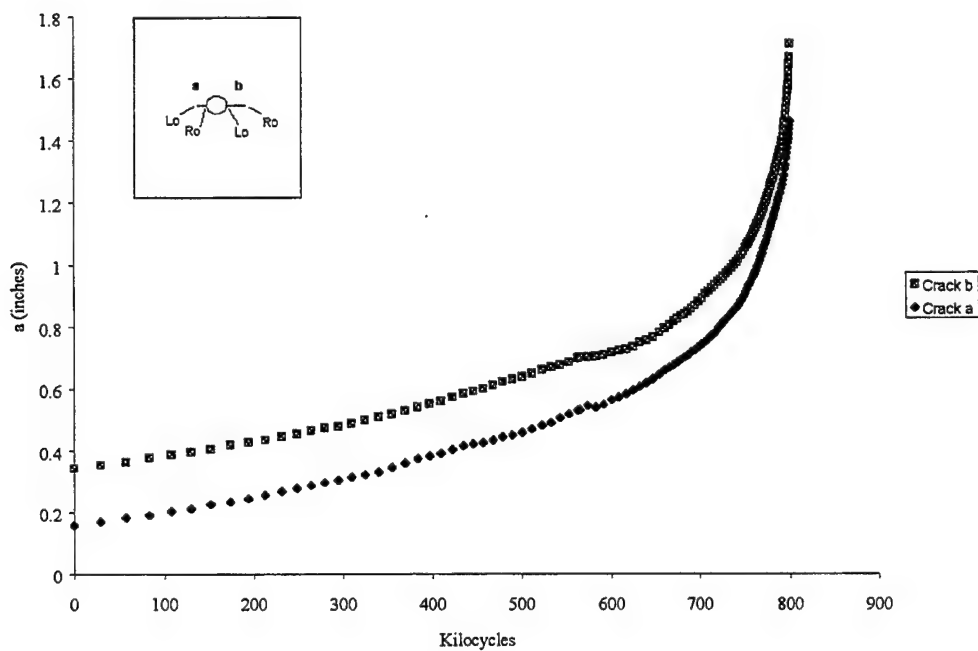

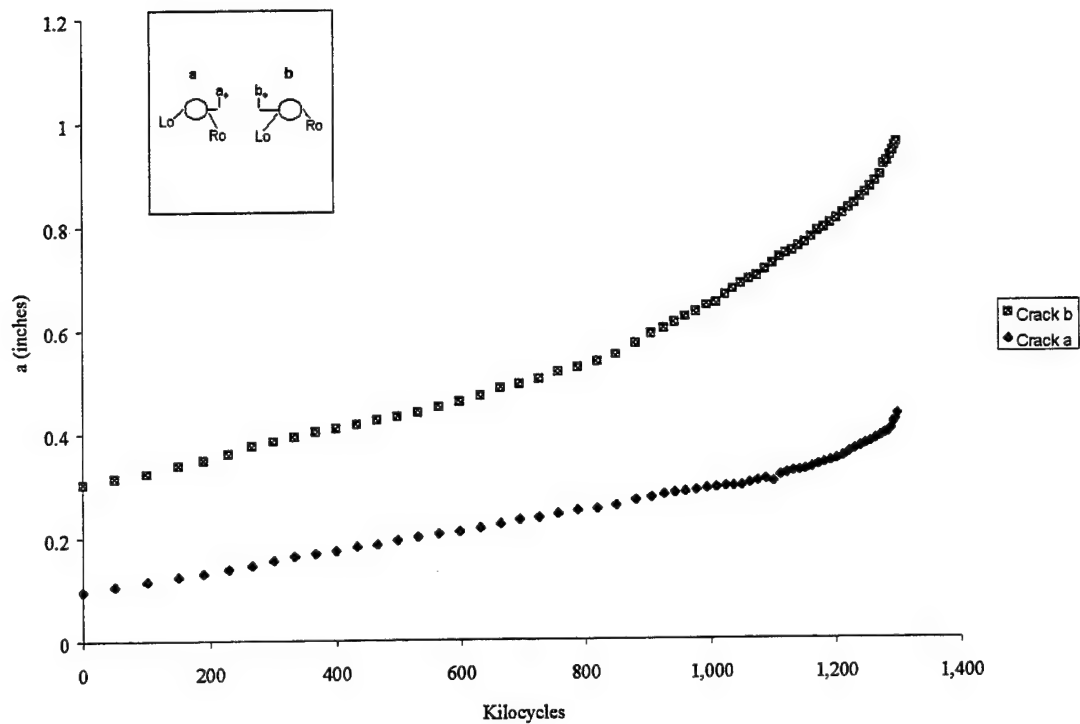**Figure 28: Crack growth plot for specimen 007-2-4 configuration B.**

22

Figure 29: Crack growth plot for specimen 007-2-5 configuration C.
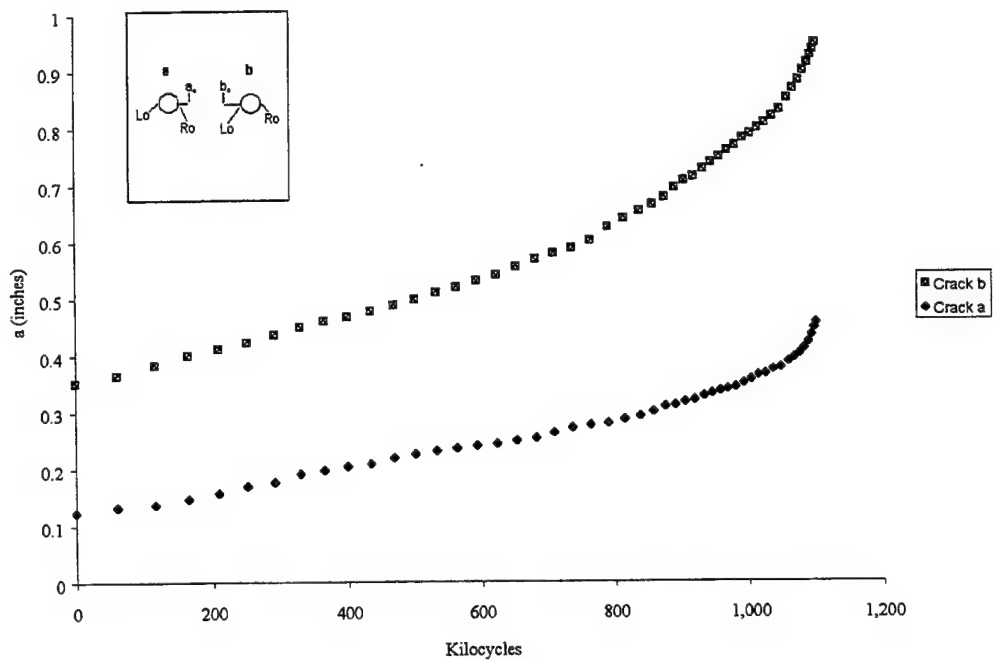

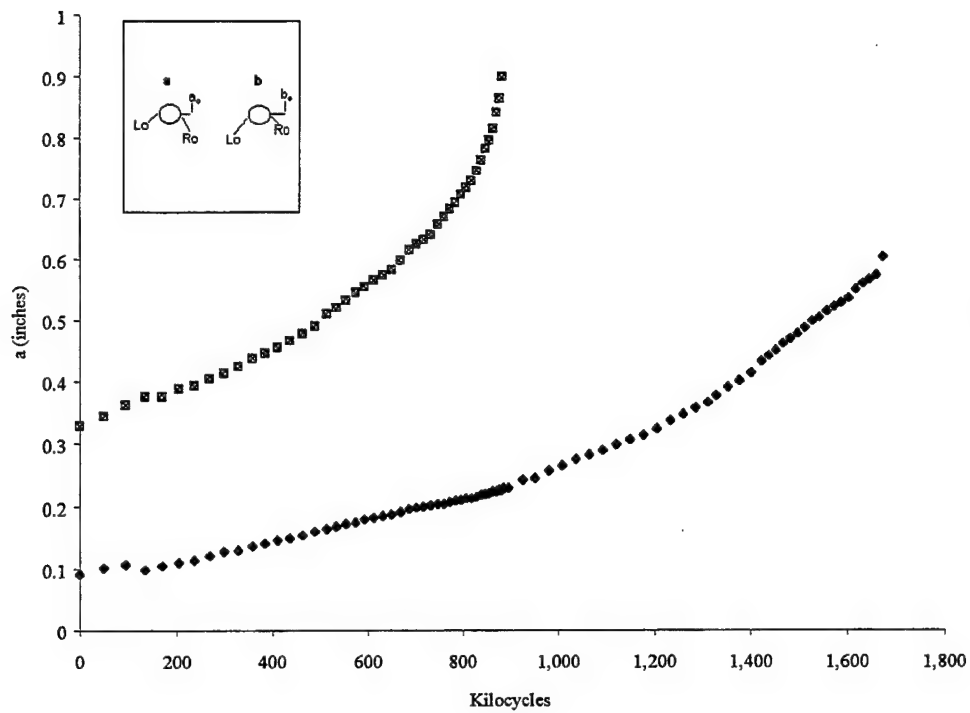**Figure 30: Crack growth plot for specimen 007-2-6 configuration C.**

23

Figure 31: Crack growth plot for specimen 007-2-7 configuration D.
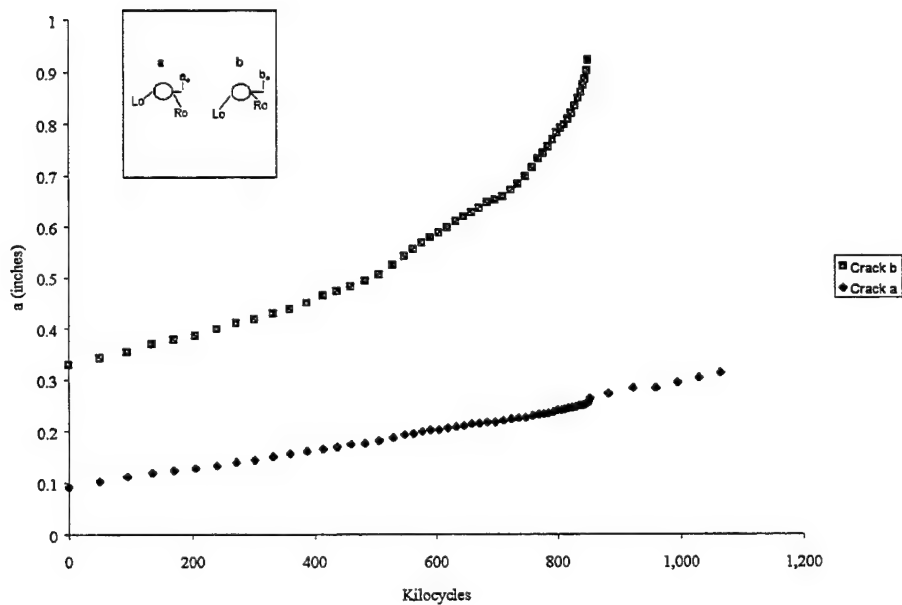

Figure 32: Crack growth plot for specimen 007-2-8 configuration D.

24

2.3   Stress Level Effects

M(T) panels (3.95 x 16 x 0.25 inches) of 7075-T73 were constant amplitude tested in dry air (relative humidity < 15%). This set of testing is a continuation of testing performed in delivery order 0002 [4]. Aluminum specimens were tested to determine the effect of mean stress levels. The humidity was not controlled and the source of the scatter of the previous data is unknown, so the current testing was conducted at RH <15% to eliminate scatter caused by humidity. Crack lengths were monitored by optical methods, and a total of 10 center-cracked specimens were tested. The test matrix is shown in Table 6. The center-cracked panels had an 0.125 inch EDM center notch machined in the center of the panel. All specimens were precracked and the precracking schedule is shown in Table 7. Crack growth rate graphs with the corresponding AFGROW curve of all tests can bee seen in Figure 33 - Figure 38. A composite of all tests, corresponding to the solid line in Figure 39, is the AFGROW da/dN vs. K_{max} curve for R= -0.33 (or any R-ratio less than -0.33). The AFGROW curve was generated from the data to be included into the AFGROW database.

Figure 33 has two sets of data points for specimen 07-03-02. The standard K solution for an M(T) specimen was used to generate the curve without the correction. The crack grew eccentrically however, so a K solution for an eccentric crack [5] was used for the corrected curve. The corrected curve is consistent with the curve of the other specimen and was used for analysis.

The data for R=-0.5 and R=-1 (Figure 33 and Figure 34, respectively) are in good agreement with the AFGROW curve. The data for R=-6 and the other high compressive loads (Figure 35 – Figure 37, respectively) however, show some deviation from the AFGROW curve. The effect is not clearly understood. The specimens were tested with the relative humidity less than 15%. If the lab air AFGROW curve for 7075-T73 is plotted on the same graph as all the data shown in Figure 38, the data lie between the two curves. So it is inconclusive if the data shifts at high compressive loading. To further illustrate this point, Figure 39 is the data for specimen 007-3-03 with the lab air and dry air AFGROW curves included. The data abruptly shifts at around ΔK=9.5 ksi√in. The humidity level reached 15% and the desiccant, which dries the chambers, was changed. After the desiccant was replaced, the crack growth rates appeared to shift once the chamber dried to a level less than 15%. Fatigue tests at humidity levels of less than 15% do not seem to definitively remove scatter.

25

Table 6: Specimen ID and test matrix for 7075-T73 tested in dry air (RH<15%).

Specimen	Max Load (kips)	Stress Ratio	Machine	Completed
07-03-01	5	-0.5	4	8/22/96
07-03-02	5	-0.5	13	9/4/96
07-03-03	5	-1	14	9/17/96
07-03-04	5	-1	13	10/11/96
07-03-05	5	-6	4	1/9/97
07-03-06	5	-6	4	1/24/97
07-03-07	22.5	-1	12	9/19/96
07-03-08	22.5	-1	12	9/20/96
07-03-09	38.6	-1	4	9/24/96
07-03-10	38.6	-1	4	9/25/96

Table 7: Precracking schedule for stress level effect specimens.

Specimens	Max Load (kips)	Stress Ratio	Half-Crack Extension
07-03-01	6.8	0	~0.005
through	5.75	0	~0.005
07-03-06	4.8	0	~0.010
07-03-07 through 07-03-10	10	0	~0.20

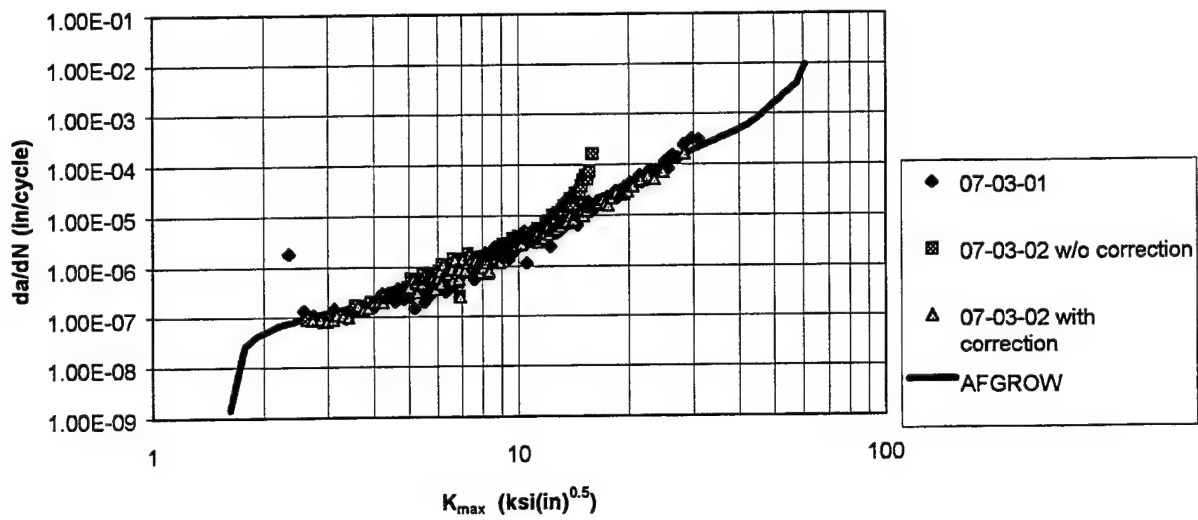**Figure 33: da/dN vs. Kmax data and AFGROW curve for Pmax = 5kips, R=-0.5.**
(w/eccentric cracking correction also included)

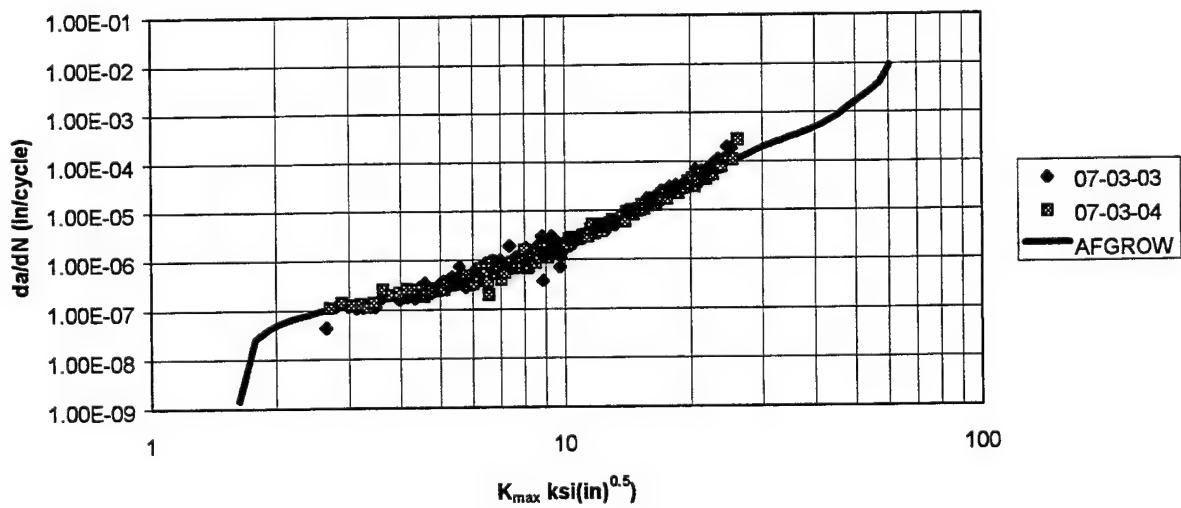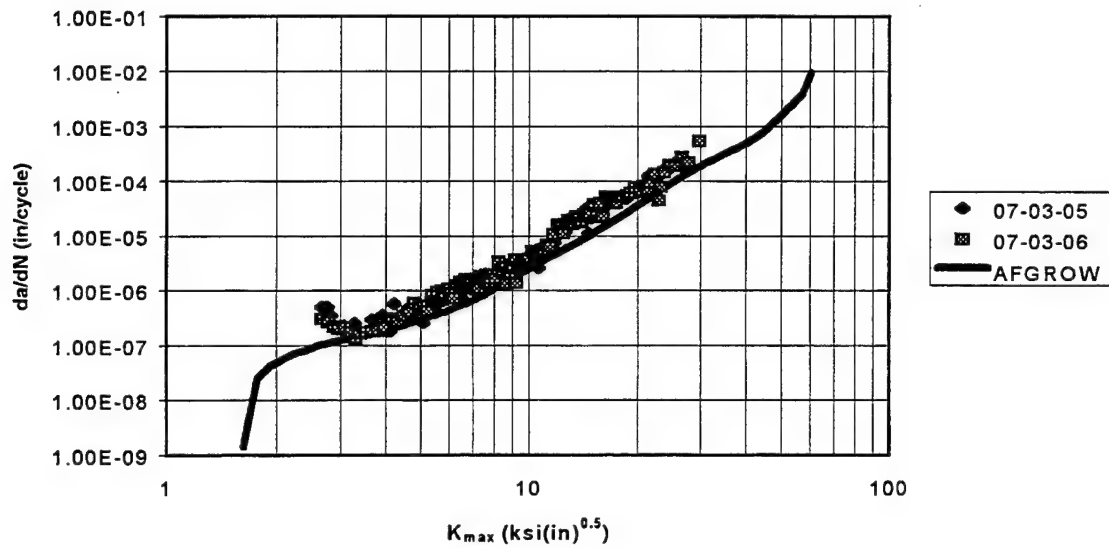**Figure 34: da/dN vs. Kmax data and AFGROW curve for Pmax = 5 kips, R=-1.**

Figure 35: da/dN vs. Kmax data and AFGROW curve for Pmax=5 kips, R=-6.

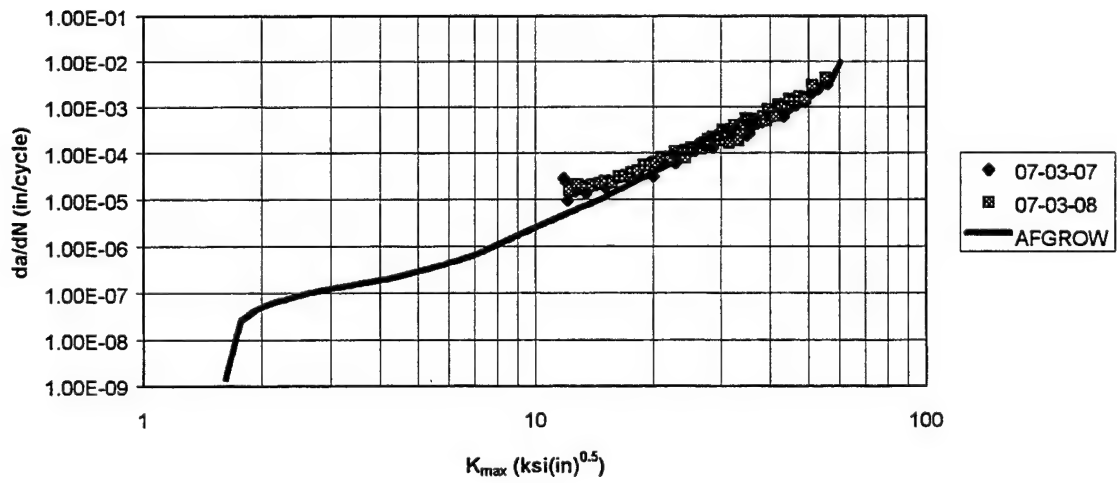**Figure 36: da/dN vs. Kmax data and AFGROW curve for Pmax=22.5 kips, R=-1.**

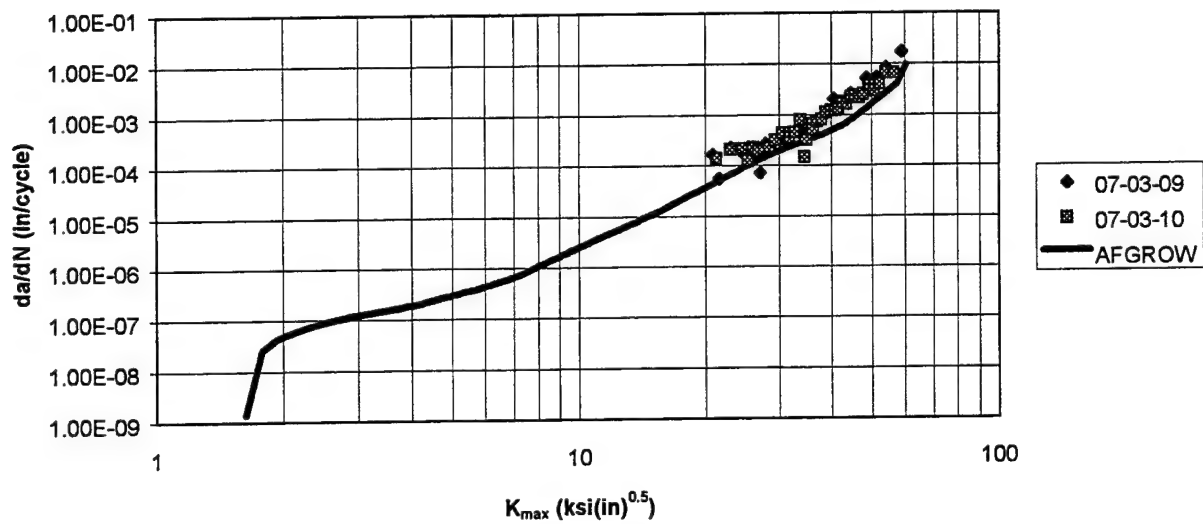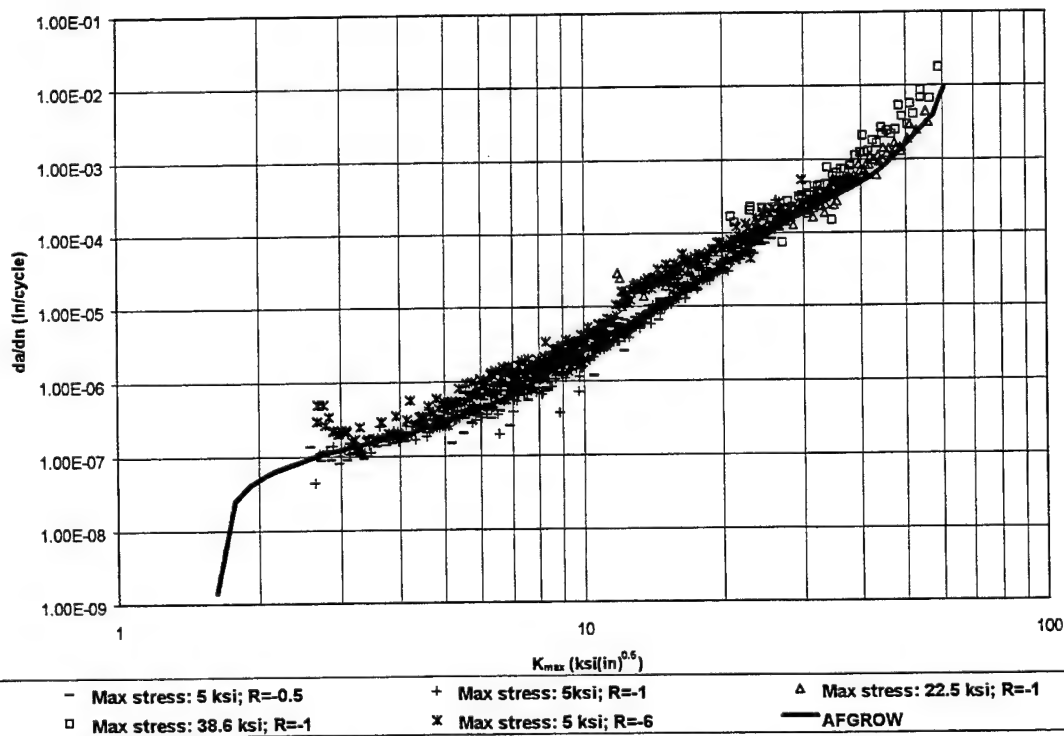**Figure 37: da/dN vs. Kmax data and AFGROW curve for Pmax = 38.6 kips, R=-1.**

Figure 38: da/dN vs. Kmax data and AFGROW curve for all specimens.
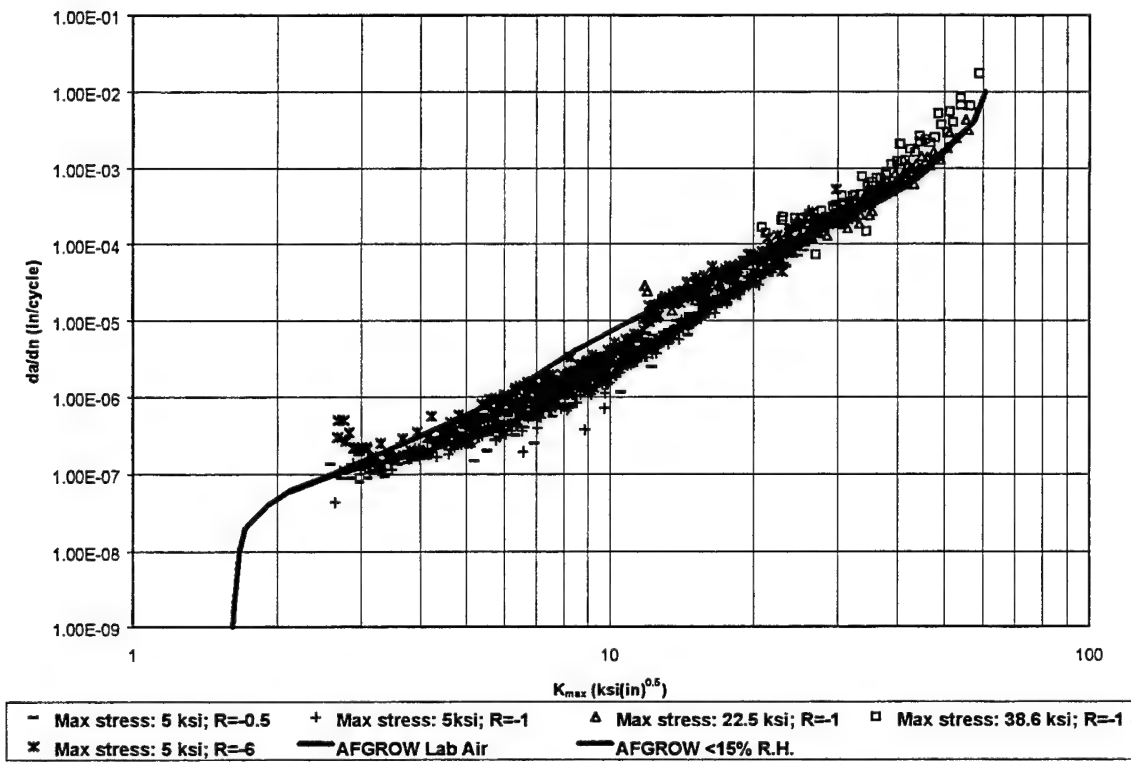**(Each data set represents two specimens)**

Figure 39: Same graph as Figure 38 with the lab air AFGROW data curve included.
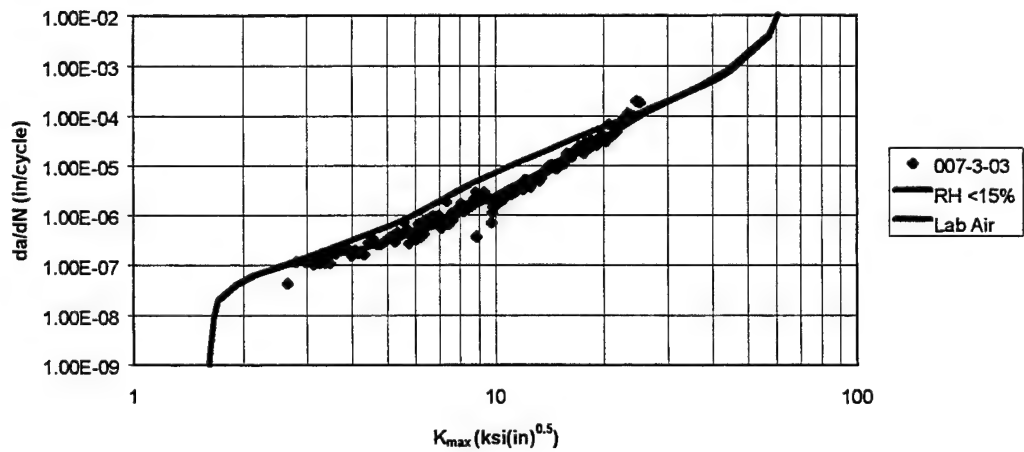

Figure 40: Data for Specimen 007-3-03 and the dry and lab air AFGROW curves.

30

2.4   Load Sequence Effects

Middle tension M(T) specimens of aluminum alloy 7075-T73 were subjected to overload, underload, overload/underload and FALSTAFF spectrum testing. The specimens were 3.95 x 0.25 x 16 inches and were precracked at 10 kips until the crack was 0.1 inch beyond the notch. All of the 1.5x spectrums were run for 1000 cycles at the nominal load and then a 50% overload or underload was applied for one cycle, and then the process was repeated. The specimens were tested with a constant load rate of 100 ksi/sec. The test matrix and lifetimes are shown in Table 8. These tests were performed to verify the closure model in AFGROW. Two specimens were tested at each condition.

Table 8: Specimen information for load sequence effects.

Specimen	Spectrum	Initial half crack size (inches)	Load (kips) nominal/over/under	Life (cycles)
007-4-1	1.5x overload	0.160	11.06/16.6/x	260,328
007-4-2	1.5x overload	0.163	11.06/16.6/x	232,232
007-4-3	1.5x underload	0.161	11.06/x/-16.6	79,079
007-4-4	1.5x underload	0.216	11.06/x/-16.6	58,058
007-4-5	1.5x over/under	0.161	11.06/16.6/-16.6	160,160
007-4-6	1.5x over/under	0.166	11.06/16.6/-16.6	140,140
007-4-7	FALSTAFF	0.167	FALSTAFF	176,611
007-4-8	FALSTAFF	0.159	FALSTAFF	183,346
007-4-control	Constant amp.	0.160	11.06/x/x	63,522

Graphs of the overload, underload, overload-underload, and falstaff tests with AFGROW predictions can be seen in Figure 40 - Figure 44, respectively. AFGROW version 3.78.1 was used using the 7075-T73 dry air data generated in the stress level effects section of this report. Other parameters include using the closure model and block cycling broken up into ten 100 cycles blocks followed by a single overload, underload, or overload underload. Various opening load ratios were used with the closure model to compare AFGROW predictions to test data. The opening load ratio did not have an effect on the underload case, but the opening load ratio did have an effect on the other three cases and the predictions are plotted with the test data. The best fitting AFGROW curve for each case uses a different opening load ratio, and more work needs to be done to understand this phenomena in order to create better prediction tools. The closure model's opening load ratio was varied to show OLRs needed to accurately predict the results. Figure 45 is a composite of all tests and it also contains the constant amplitude control specimen data.
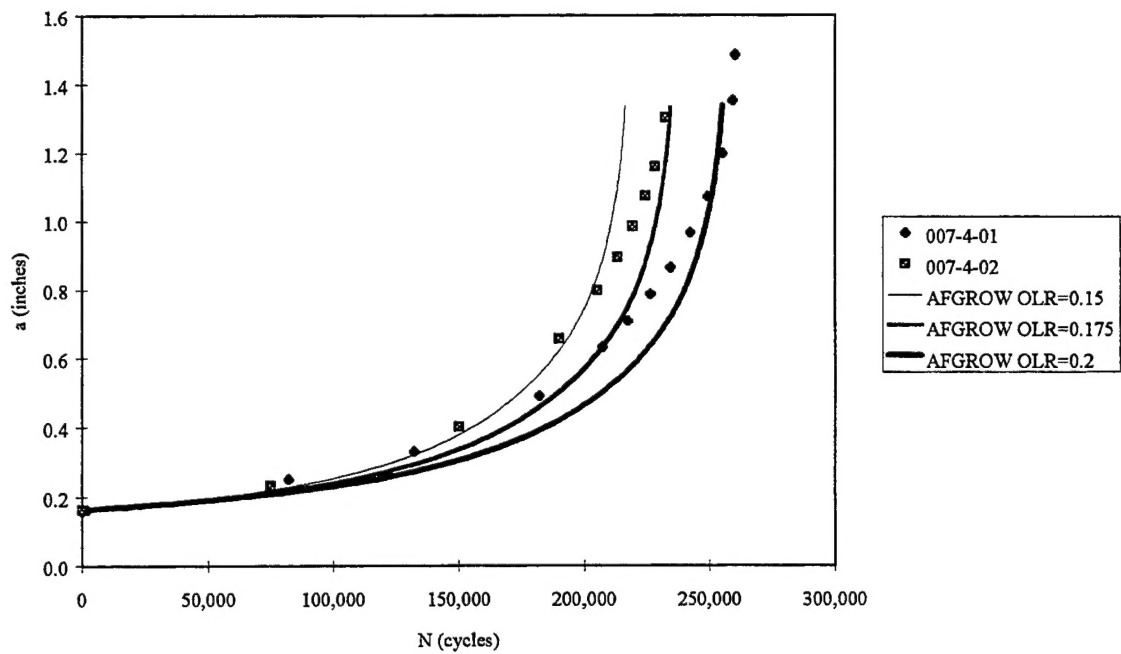
Figure 41: Crack growth plot for 1.5x overload spectrum with AFGROW prediction.
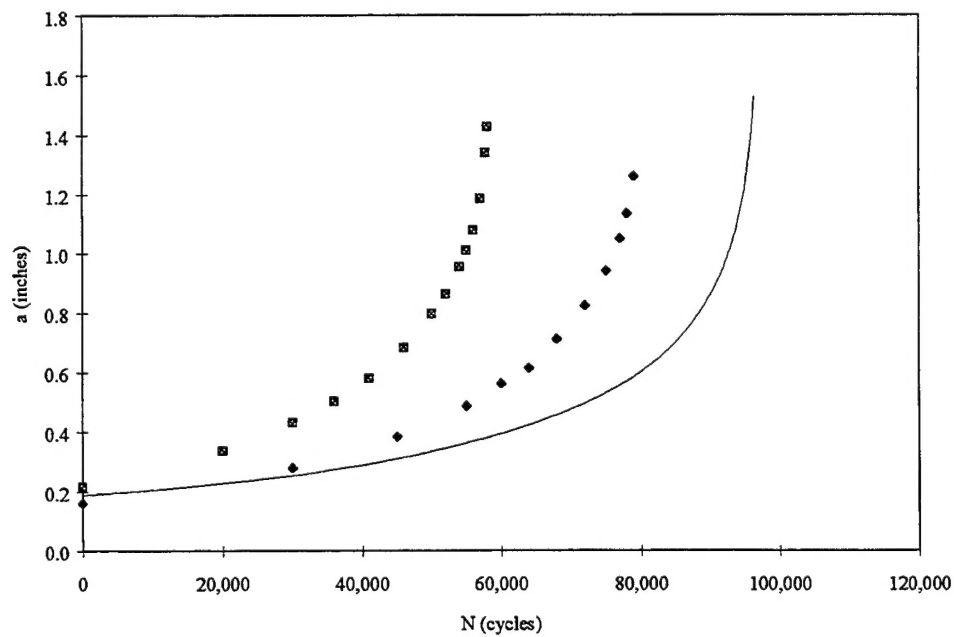

Figure 42: Crack growth plot for 1.5x underload spectrum with AFGROW prediction.
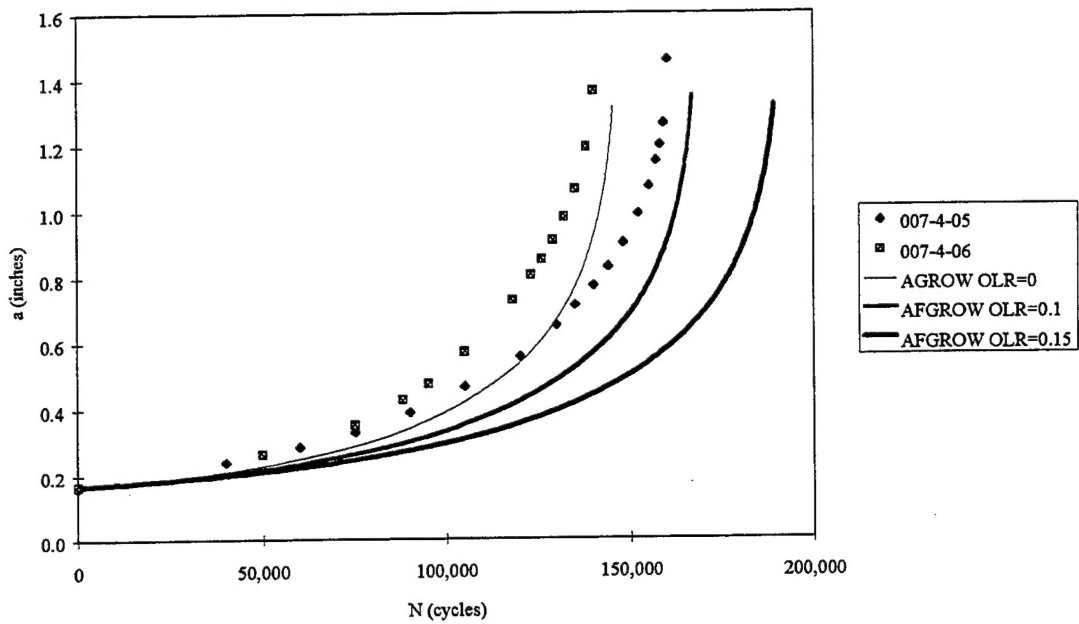
Figure 43: Crack growth plot for 1.5x overload/underload spectrum with AFGROW prediction.
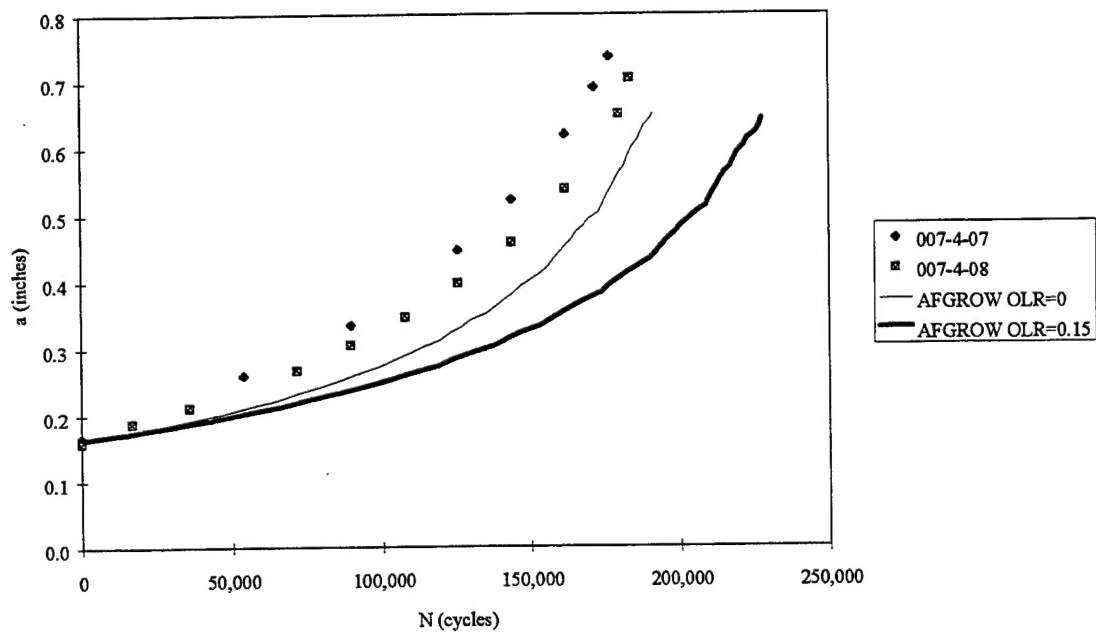

Figure 44: Crack growth plot for FALSTAFF spectrum with AFGROW prediction.

33

Load Sequence Effects of Al 7075-T73
1.5x Over/Underload @ 1000 cycles
Tested at RT & <15% RH

Legend:
● Overload Spectrum
▣ Underload Spectrum
▲ Over/Underload Spectrum
✕ FALSTAFF Spectrum
○ Control
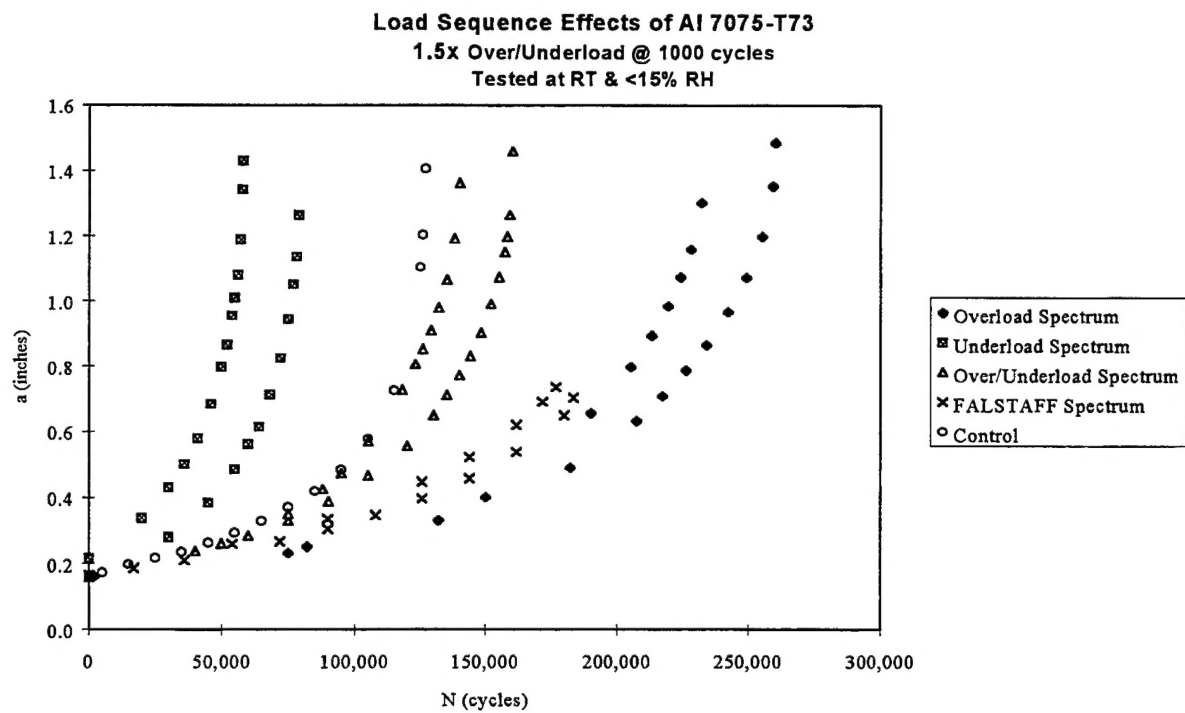
Figure 45: Composite plot of all load sequence specimens.
(with the constant amplitude control specimen included)

3. REFERENCES

[1]   "Technical Reference manual For The MATE Material Analysis And Test Environment, Version 3.x0" University of Dayton Research Institute, Dayton, OH.

[2]   K.L Boyd, J.H. Elsner, D.A. Jansen, J.A. Harter, "Structural Integrity Analysis and Verification for Aircraft Structures: Volume 2: Effects of Compressive Loading on the Fatigue Crack Growth Rates of 7075-T651 and 2024-T3 Aluminum Alloys," WL-TR-97-3017, Flight Dynacis Directorate, Wright Laboratory, Air Force Materiel Command, Wright-Patterson AFB, OH 45433-7560.

[3]   K.L. Boyd, S.Krishnan, A. Litvinov, J.H. Elsner, J.A. Harter, M.M. Ratwani, G. Glinka, "Development of Structural Integrity Analysis Technologies for Aging Aircraft Structures: Bonded Composite Patch Repait and Weight Function Methods," WL-TR-97-3105, Flight Dynamics Directorate, Wright Laboratory, Air Force Materiel Command, Wright-Patterson AFB, OH 45433-7560.

[4]   J.J. Mazza, R.J. Kuhbauder, "Understanding the Australian Silane Surface Treatment," Proc. 38th International SAMPE Symposium and Exhibition, Anaheim, California, May 1993.

[5]   M. Isida, "Stress-Intensity Factors for the Tension of an Eccentrically Cracked Strip, Trans. ASME, Ser. E, *J. Appl. Mech.*, Vol. 33 (1966), pp. 674-675.